

A THEORETICAL STUDY OF  
CARBAMATE FORMATION

By

JAMES RAY DIERS

//

Bachelor of Science

State University of New York

Stony Brook, New York

1980

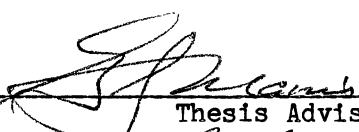
Submitted to the Faculty of the Graduate College  
of the Oklahoma State University  
in partial fulfillment of the requirements  
for the degree of  
MASTER OF SCIENCE  
December, 1986

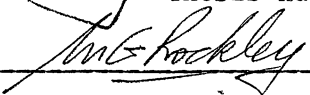
Thesis  
1986  
DS63t  
Cop. 2

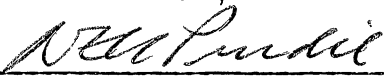


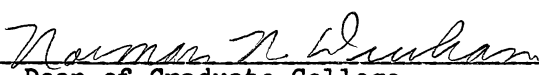
A THEORETICAL STUDY OF  
CARBAMATE FORMATION

Thesis Approved:

  
\_\_\_\_\_  
Thesis Advisor

  
\_\_\_\_\_  
Mr. Rockley

  
\_\_\_\_\_  
Neil Purdie

  
\_\_\_\_\_  
Dean of Graduate College

1263960

## ACKNOWLEDGMENTS

The advancement of science is a group effort and not that of one individual. I wish to thank a few who have made this study possible.

I wish to give special thanks to my research advisor, Dr. Gilbert J. Mains, for his advice, insight and encouragement during my study at Oklahoma State University. It has been a pleasure to share time with a man with so much enthusiasm for science. Thanks go to the members of my committee, Dr. Mark G. Rockley and Dr. Neil Purdie for consenting to serve and for their help.

Financial support from the Oklahoma State University Chemistry Department and the Gas Processing Association is gratefully acknowledged.

To my parents, Victor and Catherine Diers goes appreciation for imparting upon me a zest for knowledge. Their early encouragement to inquire has led me to a profession which I truly enjoy.

TABLE OF CONTENTS		
Chapter		Page
I.	INTRODUCTION . . . . .	1
II.	HISTORICAL . . . . .	5
III.	RESULTS AND DISCUSSION . . . . .	21
	Introduction . . . . .	21
	Geometry Calculations . . . . .	22
	Energy Calculations . . . . .	43
	Vibrational Frequency Calculations . . . . .	54
IV.	SUMMARY AND CONCLUSIONS . . . . .	59
	BIBLIOGRAPHY . . . . .	62

# LIST OF TABLES

Table	Page
I. Equilibrium Results Obtained by Christensson . . . . .	7
II. Chemical Thermodynamic Data . . . . .	14
III. Hisatsune's Infrared Band Assignments . . . . .	15
IV. Geometry and Energy Results Obtained by Pople et al. and Schafer et al. for Carbamic Acid . . . . .	19
V. Geometry and Energy Results Obtained by Pople et al. and Schafer et al. for Urea . . . . .	20
VI. HF/4-31G Optimized Geometries of $H_2$ , $N_2$ , $O_2$ and $H_2O$ . . . .	23
VII. HF/4-31G Optimized Geometry of Carbon Dioxide . . . . .	23
VIII. HF/4-31G Optimized Geometry of Ammonia . . . . .	24
IX. HF/4-31G Optimized Geometry of CIS-Carbamic Acid . . . . .	25
X. HF/4-31G Optimized Geometry of TRANS-Carbamic Acid . . . . .	26
XI. Atomic Charges on CIS and TRANS-Carbamic Acid . . . . .	27
XII. HF/4-31G Optimized Geometry of the Mono-Hydrate of CIS-Carbamic Acid . . . . .	28
XIII. Atomic Charges on Mono-Hydrate of CIS-Carbamic Acid . . . .	29
XIV. HF/4-31G Optimized Geometry of the $CO_2-NH_3$ Lewis Adduct . .	30
XV. Geometry of $CO_2-NH_3$ Lewis Adduct vs. C-N Interatomic Distance . . . . .	31
XVI. Non-Optimized Geometry of the Mono-Hydrate of the $CO_2-NH_3$ Lewis Adduct . . . . .	32
XVII. Convergence Data for the Last Point of the HF/4-31G Optimization of the Mono-hydrate of the $CO_2-NH_3$ Lewis Adduct . . . . .	33
XVIII. Atomic Charges on Atoms in Ammonia and Carbon Dioxide vs. C-N Interatomic Distance . . . . .	35

Table	Page
XIX. Eigenvalue and Eigenvector of HOMO of $\text{CO}_2\text{-NH}_3$ Lewis Adduct vs. C-N Interatomic Distance . . . . .	37
XX. Total Energies of Molecules of Interest . . . . .	44
XXI. Total Energy of the $\text{CO}_2\text{-NH}_3$ Lewis Adduct vs. C-N Interatomic Distance . . . . .	45
XXII. Geometry and Total Energy of $\text{CO}_2\text{-NH}_3$ the Lewis Adduct vs. O-C-N-H Dihedral Angle . . . . .	48
XXIII. Calculated Zero Point Energies, Thermal Energies and Entropies for Molecules of Interest . . . . .	50
XXIV. Calculated Formation Thermochemical Data . . . . .	51
XXV. Calculated Energy and Thermochemical Data for Reactions of Interest . . . . .	53
XXVI. Vibrational Frequencies of $\text{H}_2$ , $\text{N}_2$ , $\text{O}_2$ , $\text{H}_2\text{O}$ , $\text{CO}_2$ and $\text{NH}_3$ . .	55
XXVII. Calculated Vibrational Frequencies of CIS-Carbamic Acid . .	56
XXVIII. Calculated Vibrational Frequencies of TRANS-Carbamic Acid .	57
XXIX. Calculated HF/4-31G and HF/6-31G* Vibrational Frequencies of the $\text{CO}_2\text{-NH}_3$ Lewis Adduct . . . . .	58

Figure	LIST OF FIGURES	Page
1.	Concentration of Major Ionic Species When 2N MEA Reacts With Pure CO <sub>2</sub> . . . . .	9
2.	Some Possible Reaction Mechanisms for the Formation of Carbamic Acid in the Aqueous Phase . . . . .	11
3.	Reaction Mechanism Proposed by Lishnevskii and Medzievskaya for the Formation of Urea in the Gas Phase . . . . .	11
4.	Infrared Spectra of CO <sub>2</sub> /NH <sub>3</sub> /Carbamate system Obtained by Hisatsuné . . . . .	16
5.	HF/3-21G and HF/6-31G* Optimized Structures of the CO <sub>2</sub> -NH <sub>3</sub> Lewis Adduct Obtained by Amos et al. . . . .	18
6.	HOMO of Ammonia . . . . .	34
7.	LUMO of Carbon Dioxide . . . . .	34
8.	Vibrational Eigenvector Obtained for the CO <sub>2</sub> -NH <sub>3</sub> Lewis Adduct .	39
9.	HOMO of CIS-Carbamic Acid . . . . .	41
10.	HOMO of TRANS-Carbamic Acid . . . . .	42
11.	Plot of Total Energy (MP4SDQ) vs. C-N Interatomic Distance of the CO <sub>2</sub> -NH <sub>3</sub> Lewis Adduct . . . . .	46



## CHAPTER I

### INTRODUCTION

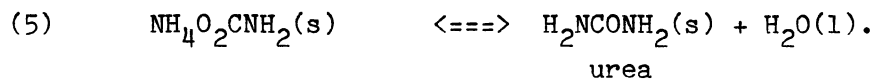
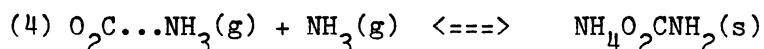
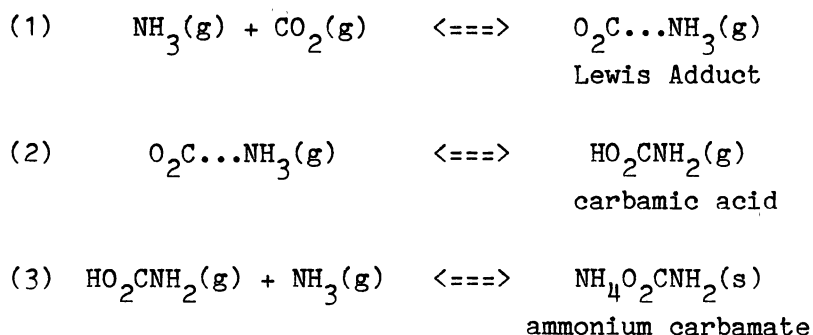
The reaction of  $\text{CO}_2$  with  $\text{NH}_3$  is of considerable theoretical as well as practical importance. The abundance of  $\text{CO}_2$  and  $\text{NH}_3$  in nature in itself indicates the importance of the interactions and the reactions of these two chemical species.

This interaction is theoretically interesting because it involves the unoccupied orbitals of  $\text{CO}_2$  and the lone pair electrons on  $\text{NH}_3$  in a Lewis type acid-base interaction. In recent years, numerous studies of systems which involve Lewis type acid-base interactions have appeared in the literature. An important class of systems which involves the interaction between a molecule with one or more electron deficient atoms and a molecule with lone pair electrons is hydrogen bonded systems. Schuster et al.(1) have recently discussed this type of interaction in hydrogen bonded systems. In addition, systems similar to  $\text{H}_3\text{N}/\text{CO}_2$ , such as  $\text{HCN}/\text{CO}_2$  and  $\text{H}_3\text{N}/\text{HCl}$  have been studied (1,2,3). One aspect of these systems that has been of particular interest is the possibility of the formation of a Van der Waals type complex, here termed the Lewis Adduct.

In the  $\text{H}_3\text{N}/\text{CO}_2$  system, the interaction, in addition to leading to a Lewis acid-base adduct, can react to form ammonium bicarbonate, ammonium carbamate and/or urea depending upon the experimental

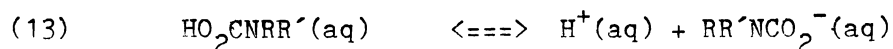
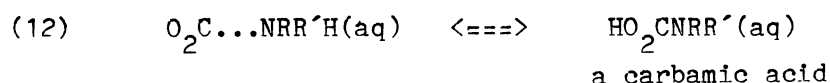
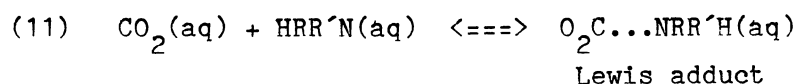
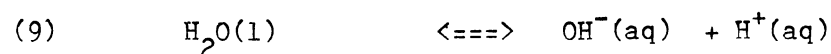
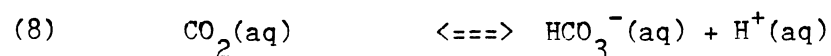
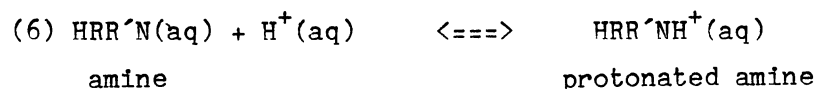
conditions. Since the  $\text{H}_3\text{N}/\text{CO}_2$  system is the simplest of the amine/ $\text{CO}_2$  systems, information obtained about this system will enable us to gain insight into the particulars of higher amine/ $\text{CO}_2$ /carbamate systems. The amine/ $\text{CO}_2$ /carbamate systems are of considerable practical importance. Carbamate formation is an important step in the commercial production of urea. More highly substituted amine/ $\text{CO}_2$ /carbamate systems include the alkanolamine/ $\text{CO}_2$ /carbamate/ $\text{H}_2\text{O}$  systems involved in the removal of  $\text{CO}_2$  from natural gas streams during processing.

The production of urea for use primarily as fertilizer is of great industrial importance. The estimated production of urea in 1984 was 6.5 million tons, with a commercial value of approximately \$1 billion (4). Urea is produced commercially on a large scale by the reaction of  $\text{CO}_2$  with  $\text{NH}_3$  at high temperature and pressure (4). Reaction conditions are in the range of 140 - 200°C and 15 - 400 atm (5). The process utilized for the manufacturing of urea involves the reaction of  $\text{CO}_2$  with  $\text{NH}_3$  to form ammonium carbamate. This process can be expressed as:



Steps (1) and (2) are investigated in this study. The question of interest here is whether or not step (2) is involved in the formation of ammonium carbamate in the gas phase. That is, is ammonium carbamate formed via steps (2) and (3) or through step (4).

The removal of acid gases, such as  $\text{CO}_2$ , from natural gas during processing is achieved through a process known as "sweetening." In the sweetening process, aqueous solutions of amines, such as monoethanolamine (MEA) or diethanolamine (DEA) react with  $\text{CO}_2$  to form carbamates (6). In aqueous solution, the amine/ $\text{CO}_2$ / $\text{H}_2\text{O}$  system can be described by the following series of equilibrium expressions:



where R and R' are defined respectively as H and H for ammonia, H and  $\text{CH}_2\text{CH}_2\text{OH}$  for MEA and,  $\text{CH}_2\text{CH}_2\text{OH}$  and  $\text{CH}_2\text{CH}_2\text{OH}$  for DEA.

In this study, details of the formation of carbamic acid in the gas phase, the monohydration of CIS-carbamic acid and the energetics of rotation about the C-N axis of the Lewis adduct are investigated. The effect of varying the C-N interatomic distance in the Lewis adduct is also studied. Using methods described in chapter III, geometries, energies and vibrational spectra of the chemical species of interest are calculated. From this data, energies of reaction and molecular orbital interactions are calculated and discussed.

## CHAPTER II

### HISTORICAL

According to Gmelin, (7) the first recorded observation of the formation of ammonium carbamate from  $\text{CO}_2$  and  $\text{NH}_3$  was in 1809. Subsequently, in 1868 Bazarov (8) discovered that ammonium carbamate yields urea upon heating under pressure. However it was not until 1922 that these two discoveries were applied to the commercial production of urea.

Several early studies concentrated on the gas phase equilibria involved in the formation of urea from  $\text{CO}_2$  and  $\text{NH}_3$  with emphasis on their temperature and pressure dependence. Briggs and Migrdichian (9) studied the first equilibria step, the formation of ammonium carbamate from ammonia and carbon dioxide. Other researchers examined this equilibrium reaction by analyzing the reverse process, the decomposition of ammonium carbamate (10,11,12). That is, they measured the vapor pressure above solid ammonium carbamate at various temperatures. Edgar et al. (12) published the following expression for the vapor pressure above solid ammonium carbamate:

$$\log P(\text{mm Hg}) = -2741.9/T(\text{ }^\circ\text{C}) + 11.1448$$

This expression is valid over the range 35 - 83°C and also agrees well with the measurements made by Briggs and Migrdichian.

Equilibrium constants for aqueous phase reactions in the carbamate system have been investigated by Fenton (13), Lewis and Burrows (14), Christensson et al. (15), Faurholt (16) and others. Due to the lack of data on the acid strength of carbamic acid, the early studies of Fenton and Lewis and Burrows were inconclusive. Faurholt investigated the aqueous carbamate system in greater detail. He experimentally determined the equilibrium expression:

$$K_1 = \frac{[\text{NH}_3] [\text{HCO}_3^-]}{[\text{H}_2\text{NCO}_2^-]}$$

to have the value  $\log K_1 = -0.48$  at 0 C and to be approximately 25% higher at 18 C.

Christensson et al., using equilibrium expressions and mass and proton balance equations, solved for the equilibrium constants of  $K_1$  and  $K_2$ , the dissociation constant for carbamic acid:

$$K_2 = \frac{[\text{H}^+] [\text{H}_2\text{NCO}_2^-]}{[\text{H}_2\text{NCO}_2^-]}$$

The values for  $pK_1$  and  $pK_2$  obtained by Christensson are given in Table I. It is evident from the data in Table I that the carbamate in aqueous solution exists primarily as the dissociated carbamic acid.

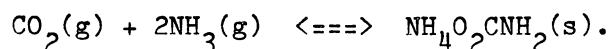
Van Krevelen et al. (17), Edwards et al. (18) and Beutier and Renon (19) have modeled the gas/aqueous two phase system of  $\text{NH}_3/\text{CO}_2/\text{H}_2\text{O}$ , incorporating activity and fugacity corrections to the equilibria expressions. These studies model the  $\text{NH}_3/\text{CO}_2/\text{H}_2\text{O}$  system of

TABLE I  
EQUILIBRIUM RESULTS OBTAINED  
BY CHRISTENSSON

T(°C)	pK1	pK2
25	-.328	6.76
35	-.288	6.61
50	-.183	6.56
70	-.079	6.49

the sour gas stripping process, which is very similar to the alkanolamine/ $\text{CO}_2/\text{H}_2\text{O}$  systems associated with sour gas sweetening of natural gas streams during processing. Figure 1 illustrates the aqueous phase composition as a function of the mole ratio of  $\text{CO}_2$  to MEA in solution. Since these two systems are similar, a plot for the  $\text{CO}_2$ /aqueous  $\text{NH}_3$  system should have the same general shape. Notice that the carbamate curve contains a maximum at  $\text{CO}_2/\text{MEA} = .5$ , which corresponds to the  $\text{CO}_2/\text{MEA}$  ratio of the protonated amine-carbamate salt. As the  $\text{CO}_2/\text{MEA}$  mole ratio increases above .5, the excess  $\text{CO}_2$  is converted to carbonic acid, which then dissociates into the bicarbonate and a proton. As the concentration of  $\text{H}^+$  increases in the solution the equilibrium associated with the amine protonation such that more protonated amine is produced.

Relatively few studies have explored the mechanism by which  $\text{CO}_2$  and  $\text{NH}_3$  combine to yield ammonium carbamate. The early gas phase studies typically present the formation of ammonium carbamate as:



Intermediate steps, such as the formation of a Lewis adduct, have only recently been suggested or explored. Currently no evidence exists for the presence of carbamic acid in the gas phase reaction yielding ammonium carbamate. Yoshida (20) has suggested that the formation of ammonium carbamate in the gas phase does not occur in the absence of water. He proposed that the reaction occurs via the initial formation of an  $\text{H}_2\text{O}-\text{NH}_3$  species which then reacts with  $\text{CO}_2$ . This is consistent with most of the observations found in the literature. Gmelin (7)



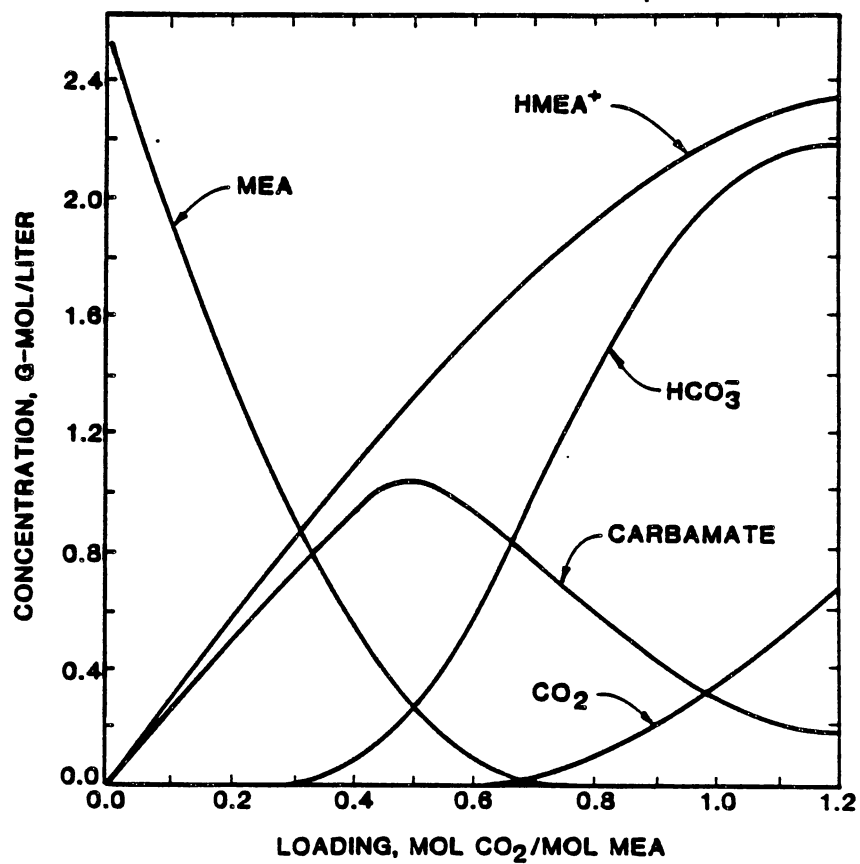


Figure 1. Concentration of Major Ionic Species When 2N MEA Reacts With Pure CO<sub>2</sub>

states that a dry  $2\text{NH}_3 + \text{CO}_2$  mixture reacts slowly at  $18^\circ\text{C}$ , but upon further drying of the initial gases, no reaction is observed in a 24 hour period. Lishnevskii and Madzievskaya (8) reject the idea that water vapor is required in the formation of ammonium carbamate. They observed that the initial rate of ammonium carbamate formation is high in a 1:1:1  $\text{NH}_3\text{-CO}_2\text{-H}_2\text{O}$  system and it is then slowly converted to the bicarbonate. This agrees with the measurements made by Faurholt (16,21). Faurholt observed that addition of  $\text{CO}_3^{=}$  to an aqueous ammonia solution produced carbamate at a rate which suggests the carbonate is first converted to aqueous  $\text{CO}_2$  before reaction to yield the carbamate. These observations enhance Yoshida's opinion, since the presence of water appears to be necessary for the gas phase reaction to proceed, and it is not necessary for bicarbonate formation. If the formation of ammonium carbamate in the gas phase requires water, the reaction in aqueous phase is likely to be similar. The obvious differences between the reaction in the aqueous system as opposed to that in the non-aqueous system lie primarily in the enhanced stability of dissociated ions in solution due to ion solvation. Also, in the aqueous phase, the presence of  $\text{H}_2\text{O}$  surrounding the  $\text{H}_3\text{N}\cdots\text{CO}_2$  Lewis adduct may enhance the conversion to carbamic acid through proton transfer. A process such as that shown in Figure 2 may occur.

Lishnevskii and Madzievskaya proposed another mechanism for the formation of ammonium carbamate. Their mechanism proceeds through the adsorption of one or more reactants on a surface, then the formation of a Lewis adduct, followed by the formation of a zwitterion and carbamic acid. The mechanism they propose is shown in Figure 3. It should be noted that all the species involved in this study are part of the

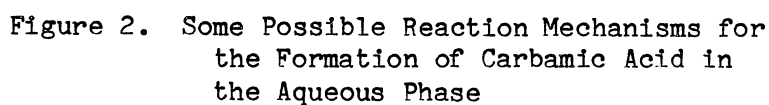


Figure 2. Some Possible Reaction Mechanisms for the Formation of Carbamic Acid in the Aqueous Phase

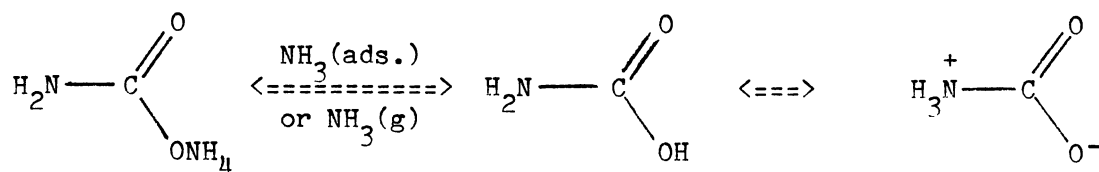
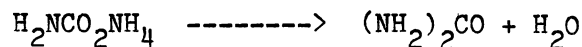


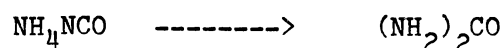
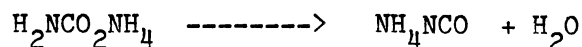
Figure 3. Reaction Mechanism Proposed by Lishnevskii and Madzievskaya for the Formation of Urea in the Gas Phase

Lishnevskii and Madzievskaya mechanism.

Two Mechanisms have been proposed for the decomposition of ammonium carbamate to form urea and water. They are:

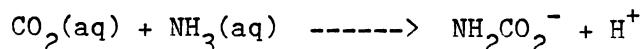


or



One reaction proceeds directly from ammonium carbamate while the other forms ammonium cyanate as an intermediate (22,23). Currently, there is no evidence for the existence of ammonium cyanate during the forward reaction. This pathway is proposed on the basis of the formation of ammonium cyanate in the reverse reaction due to urea hydrolysis (22). Also it should be noted that there is no conclusive evidence for the direct pathway being correct.

Pinsent and coworkers (24) have measured the rate and the activation energy for the reaction:



Upon applying simple collision theory to their reaction rate data, they arrived at the following Arrhenius type equation:

$$K' = 10^{11.13} \exp(-11600/RT).$$

This corresponds to an activation energy of 11.6 Kcal/mol for the

forward reaction. The activation energy for the decomposition of solid ammonium carbamate has been measured to be 11.0 and 12.4 Kcal/mol for the forward and reverse reactions, respectively (8,25).

The thermodynamics of the formation of urea from ammonia and carbon dioxide has been studied. Thermodynamic data at standard temperature and pressure are presented in Table II. Pinsent's research group (24) measured the heat of reaction directly using calorimetric methods, while the data presented by Lishnevskii and Madzievskaya were calculated from enthalpy and entropy of formation data. The values for  $\Delta G^\circ(298)$  and  $\ln K_p^\circ$  are calculated from  $\Delta H^\circ$  and  $\Delta S^\circ$  data given in the reference stated using the equations:

$$\Delta G^\circ = \Delta H^\circ - T\Delta S^\circ$$

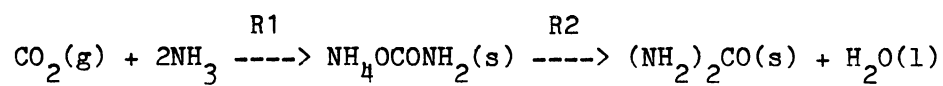
$$K_p^\circ = \exp(-\Delta G^\circ/RT)$$

As can be seen from the data in Table II, the formation of ammonium carbamate is favored at 298°K while its decomposition into urea and water is not.

Frasco (26) and Hisatsune (27) have studied the formation of ammonium carbamate at low temperature through the use of infrared spectroscopy. The earlier work of Frasco was re-examined by Hisatsune who reassigned peaks originally thought to be associated with amorphous and crystalline ammonium carbamate to the unstable precursor  $(\text{NH}_3)_2\text{CO}_2$ . In Table III and Figure 4 the spectra obtained by Hisatsune and peak assignments are shown. Klemperer et al. (28,29) have measured and analyzed the microwave spectra of several weakly bonded ammonia

TABLE II

## CHEMICAL THERMODYNAMIC DATA



Reaction	$\Delta\text{H}^\circ(\text{Kcal/mol})$	$\Delta\text{S}^\circ(\text{e.u.})$	$\Delta\text{G}^\circ(\text{Kcal/mol})$	$\ln K_p^\circ$	ref.
R1	-38.32	-103.43	-7.48	+12.6	8
R1	-36.30	- - - -	- - -	- - -	24
R1	-37.80	- - - -	- - -	- - -	43
R1	-38.09	-111.09	-4.91	+ 8.29	44
R2	+ 6.26	+ 2.03	+5.65	- 9.54	8
R2	+ 6.15	+ 9.80	+3.22	+5.53	44

TABLE III

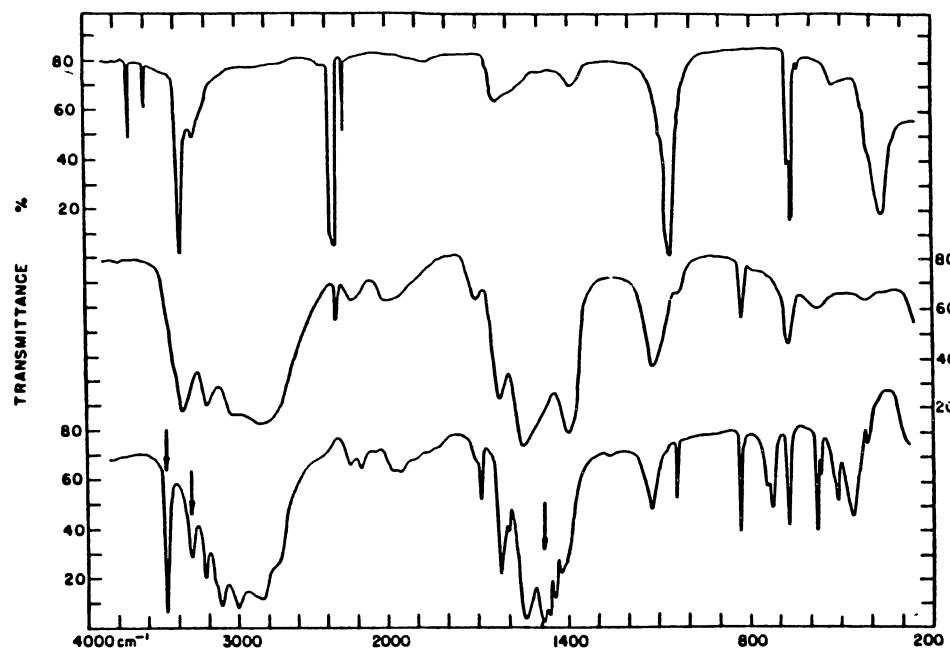
## HISATSUNE'S INFRARED BAND ASSIGNMENTS

Infrared spectra of ammonium carbamate and its precursor at  $-190^{\circ}\text{C}$  ( $\text{cm}^{-1}$  units)

Assignments <sup>a</sup>	$(\text{NH}_4)_2\text{CO}_3$	$(\text{ND}_4)_2\text{CO}_3$	$\text{NH}_4^+\text{NH}_2\text{CO}_2$	$\text{NH}_4^+\text{ND}_2\text{CO}_2$	Assignments <sup>a</sup>
$\nu_s(\text{NH}_4)$	3370	2510	3475 <sup>b</sup>	2600 <sup>b</sup>	$\nu_s(\text{NH}_2)$
$\nu_s(\text{NH}_4)$	3220	~2340	3310 <sup>b</sup> 3220 3120	2430 <sup>b</sup> ~2330 2250	$\nu_s(\text{NH}_2)$
	~3030	~2240			
	~2850	~2140	3010 ~2830 ~2750	2183 2125 ~2070	$\nu(\text{NH}_4^+)$
	~2240	~1650	2240 2170		
	~1975		~1970		
	~1710		1680		
$\delta_s(\text{NH}_4)$	1625	1210 ~1180	1625	1232 1200	$\delta(\text{NH}_2)$
				1174 1158 1150	$\delta(\text{NH}_4^+)$
$\nu_s(\text{CO}_2)$	1545 ~1490	1530	1545	1527	$\nu_s(\text{CO}_2)$
			1485 <sup>b</sup> 1464 1447	1072 <sup>b</sup> ~1052	$\delta(\text{NH}_4^+)$
$\nu_s(\text{CO}_2)$	1400	1435	1425	~1450 1390 1367 1000 990	$\nu_s(\text{CO}_2)$
			1265 1122	915 1117 ~1100	$\rho(\text{NH}_2)$ $\nu_s(\text{CN})$
$\nu(\text{CN})$	1120	1130 ~1080			
$\delta_s(\text{NH}_4)$		.910	1040	~810	$\omega(\text{NH}_2)$
$\delta_s(\text{NH}_4)$		860			
$\omega(\text{CO}_2)$	830	827	832 745 728	826 ~700	$\omega(\text{CO}_2)$ $\rho(\text{CO}_2)$
$\delta(\text{CO}_2)$	680	665	670	657	$\delta(\text{CO}_2)$
$\tau(\text{CO}_2)$	~580	~500	580 567	537 510 ~440 ~390	$\tau(\text{CO}_2)$
			512 460	364 342	$\text{L}(\text{NH}_4^+)$

<sup>a</sup> $\nu_u$  = antisymmetric stretch,  $\nu_s$  = symmetric stretch,  $\delta$  = deformation,  $\omega$  = wag,  $\rho$  = rock,  $\tau$  = torsion, and L = lattice.

<sup>b</sup>These peaks are identified by arrows in Figs. 1 and 2.



. Infrared spectra of  $\text{NH}_3/\text{CO}_2 = 3.0$  system at  $-190^\circ\text{C}$ . Top spectrum, initial; central spectrum, after warming to  $-100^\circ\text{C}$ ; lower spectrum, after warming to  $-25^\circ\text{C}$ . Arrows indicate characteristic  $\nu(\text{NH}_3)$  and  $\delta(\text{NH}_3^+)$  absorption bands.

Figure 4. Infrared Spectra of  $\text{CO}_2/\text{NH}_3/\text{Carbamate}$  System  
Obtained by Hisatsune (27)



complexes including that of  $O_2C...NH_3$ . Klemperer's group calculated the C-N interatomic distance to be 2.9875Å.

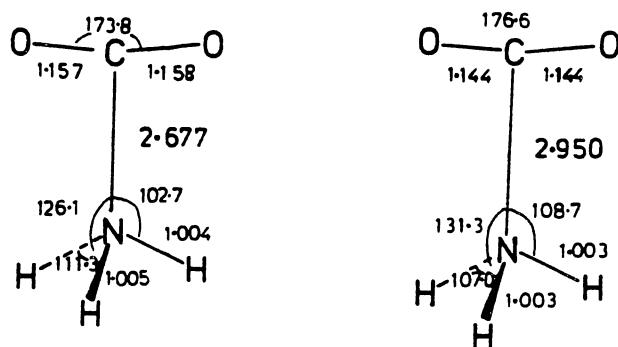
Amos and coworkers (30) made ab initio molecular orbital calculations of the  $O_2C...NH_3$  Lewis adduct at the HF/3-21G and HF/6-31G\* level. The optimized structures they obtained are shown in Figure 5. The longer C-N interatomic distance calculated by HF/6-31G\* agrees well with the experimental value obtained by Klemperer.

Pople et al. (31) using "standard" bond angles and bond lengths have calculated the HF/4-31G total energies of carbamic acid and urea to be -152758.49 and -165183.52 Kcal/mol, respectively. The "standard" bond angles and bond lengths used for these single point calculations were determined from average values by a method described in reference (32). The structures obtained for carbamic acid and urea are shown in Tables IV and V, respectively.

Schafer and coworkers (33) performed geometry optimization calculations for carbamic acid and urea at the HF/4-21G level. The results obtained from these calculations are shown in Tables IV and V.

The results of both Schafer's and Pople's groups indicate that the TRANS form of carbamic acid is the lower energy structure. In both studies, a planar geometry was found for carbamic acid.

3-21G STRUCTURE      6-31G\* STRUCTURE

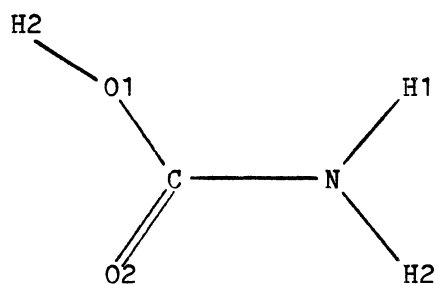


BOND LENGTHS (Å)  
BOND ANGLES (°)

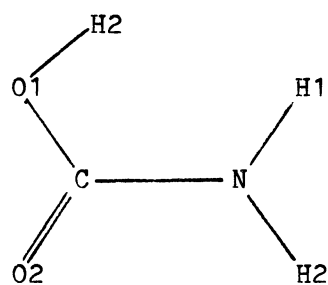
Figure 5      HF/3-21G and HF/6-31G\* Optimized Structures  
of the  $\text{CO}_2\text{-NH}_3$  Lewis Adduct

TABLE IV

GEOMETRY AND ENERGY RESULTS OBTAINED BY POPLE ET AL.  
AND SCHAFFER ET AL. FOR CARBAMIC ACID



TRANS



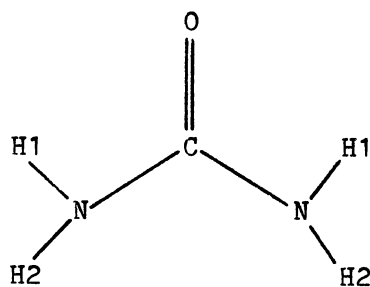
CIS

	Schafer		Pople	
	CIS	TRANS	CIS	TRANS
C-N	1.3657	1.3455	1.32	1.32
O1-C	1.3716	1.3695	1.36	1.36
O1-H2	.9609	.9628	.96	.96
O2-C	1.2026	1.2113	1.36	1.36
N-H1	.9920	.9917	1.01	1.01
N-H3	.9937	.9918	1.01	1.01
H2-O1-C	115.94	110.64	109.47	109.47
O1-C -O2	120.79	122.91	120.0	120.0
O1-C -N	114.68	109.93	120.0	120.0
O2-C -N	124.53	127.17	120.0	120.0
H1-N -C	124.19	120.17	120.0	120.0
H3-N -C	117.29	119.14	120.0	120.0
H1-N -H3	118.53	120.69	120.0	120.0
H2-O1-C -N	0.0	180.0	0.0	180.0
E(HF) Kcal/mol	-152619.02	-152629.71	-152758.49	-152747.17

UNITS = Angstroms and Degrees

TABLE V

GEOMETRY AND ENERGY RESULTS OBTAINED BY  
POPLE ET AL. AND SCHAFER ET AL.  
FOR UREA



UREA

	Schafer	Pople
C-N	1.3680	1.32
N-H1	.9924	1.01
C-O	1.2231	1.36
N-H2	.9924	1.32
N -C -N	114.54	120.
O -C -N	122.73	120.
H1-N -H2	119.12	120.
H1-N -C	117.29	120.
H2-N -C	119.12	120.
E(HF)Kcal/mol	-140220.81	-140343.79

UNITS = Angstroms and Degrees

## CHAPTER III

### RESULTS AND DISCUSSION

#### Introduction

Ab initio molecular orbital calculations were performed with the Gaussian 82 system of programs developed by Pople and colleagues at Carnegie- Mellon University (34). The potential energy surface was explored using the 4-31G split valence basis set (35). The Lewis adduct of  $\text{CO}_2$  and  $\text{NH}_3$  was also investigated using the 6-31G\* split valence basis set (36). 4-31G utilizes inner shell expansions of four gaussian functions and two valence shells comprising three and one gaussian, respectively. 6-31G\* utilizes inner shell expansions of six gaussian functions and two valence shells comprising three and one gaussian, respectively, and incorporates d functions.

With the exception of the Lewis adduct of  $\text{CO}_2$  and  $\text{NH}_3$ , all equilibrium geometries were fully optimized using numerical gradient methods at the Hartree-Fock level (37). The geometry of the  $\text{NH}_3\text{-CO}_2$  Lewis adduct was determined using analytical gradient methods at the Hartree-Fock level (40). All optimized geometries were verified using analytical gradient methods during calculations employing the frequency analysis portion of the Gaussian 82 program. Electron correlation energy has been estimated using Moller-Plesset theory up to the fourth order, including single, double and quadruple excitations at the

Hartree-Fock optimized geometry (MP4SDQ/4-31G//HF/4-31G, frozen core) (38,39). Vibrational frequencies and zero point energies were obtained from analytical derivatives calculated at the Hartree-Fock optimized geometry (40). Thermal contributions include 1/2 RT for each translational or rotational degree of freedom and changes in vibrational or rotational energy due to the thermal population of excited modes.(41) In the calculation of zero point energies, the contributions from imaginary frequencies are ignored.

#### Geometry Calculations

Fully optimized HF/4-31G geometries for  $H_2$ ,  $N_2$ ,  $O_2$ ,  $H_2O$ ,  $CO_2$ ,  $NH_3$ , CIS- $H_2NCO_2H$ , TRANS- $H_2NCO_2H$ , and  $H_2O \cdot CIS-H_2NCO_2H$  are given in Tables VI thru X and XII. Table XI lists the atomic charges in CIS and TRANS-carbamic acid and Table XIII lists the atomic charges in the mono-hydrate of CIS-carbamic acid. The optimized geometry for the  $H_3N-CO_2$  Lewis adduct is given in Table XIV. Table XV presents the optimized geometry of the Lewis adduct as a function of fixed C-N interatomic distance. The non-optimized geometry for  $H_2O \cdot O_2C \cdots NH_3$  is shown in Table XVI. This  $H_2O \cdot O_2C \cdots NH_3$  geometry is the last in an incomplete optimization run. The convergence tolerance values for this last point are given along with the convergence criterion in Table XVII.

The interaction between the HOMO of  $NH_3$  and the LUMO of  $CO_2$  is pictorially presented in Figures 6 and 7. Atomic charges for N, H, C and O in  $NH_3$  and  $CO_2$  are listed in Table XVIII (C-N = infinity). It can be seen from the results given in Table XVIII that the difference in electronic charges of carbon in carbon dioxide and nitrogen in

TABLE VI

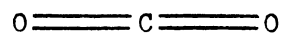
HF/4-31G OPTIMIZED GEOMETRIES OF  
H<sub>2</sub>, N<sub>2</sub>, O<sub>2</sub> AND H<sub>2</sub>O

Molecule	Calculated		Experimental*	
	Bond Distance	Bond Angle	Bond Distance	Bond Angle
H2	.7297	- - -	.7415	- - -
N2	1.0847	- - -	1.0976	- - -
O2	1.1963	- - -	1.2074	- - -
H2O	.9505	- - -	.9572	104.5

UNITS = Angstroms and Degrees  
\* ref. (45)

TABLE VII

HF/4-31G OPTIMIZED GEOMETRY  
OF CARBON DIOXIDE

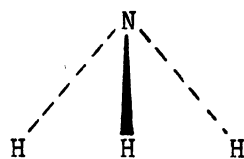


	Calculated	Experimental*
C - O	1.1576	1.1618
O - C - O	180.	180.

UNITS = Angstroms and Degrees  
\* ref. (45)

TABLE VIII

HF/4-31G OPTIMIZED GEOMETRY OF AMMONIA



	Calculated	Experimental*
N - H	.9911	1.016
H - N - H	115.832	107.3

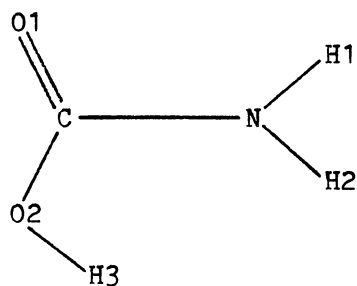
UNITS = Angstroms and Degrees

\* ref. (45)



TABLE IX

HF/4-31G OPTIMIZED GEOMETRY OF CIS-CARBAMIC ACID

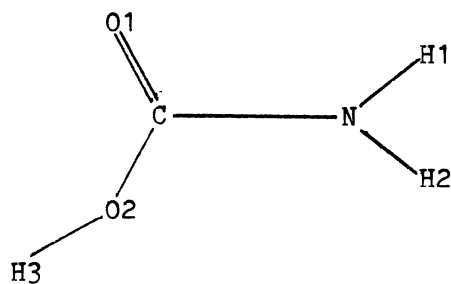


Bond Distance		Bond Angle	
O1-C	1.2050	O1-C -O2	120.5873
O2-C	1.3552	C -O2-H3	118.1694
H3-O2	0.9504	O2-C -N	115.3877
C -N	1.3557	H1-N -C	124.2909
H1-N	0.9906	H1-N -H2	118.1664
H2-N	0.9890	H2-C -N	117.5427
		O1-C -N	124.0251

UNITS = Angstroms and Degrees

TABLE X

HF/4-31G OPTIMIZED GEOMETRY OF TRANS-CARBAMIC ACID

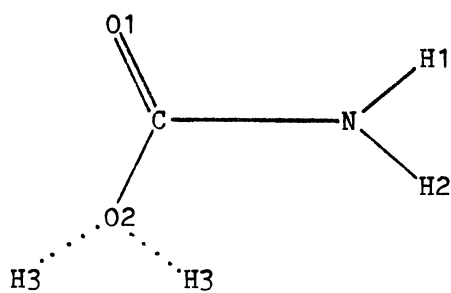


Bond Distance		Bond Angle	
O1-C	1.2155	O1-C -O2	122.5600
O2-C	1.3518	C -O2-H3	112.7607
H3-O2	0.9529	O2-C -N	111.1915
C -N	1.3368	H1-N -C	119.1148
H1-N	0.9893	H1-N -H2	120.1055
H2-N	0.9892	H2-C -N	120.7797
		O1-C -N	126.2485

UNITS = Angstroms and Degrees

TABLE XI

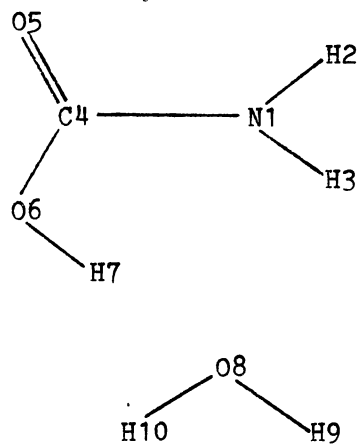
ATOMIC CHARGES ON CIS AND TRANS-CARBAMIC ACID



Atom	CIS	TRANS
C	+1.07	+1.03
N	-0.93	-0.90
O1	-0.60	-0.63
O2	-0.73	-0.74
H1	+0.40	+0.39
H2	+0.37	+0.40
H3	+0.43	+0.45

TABLE XII

HF/4-31G OPTIMIZED GEOMETRY OF THE  
MONO-HYDRATE OF CIS-CARBAMIC ACID

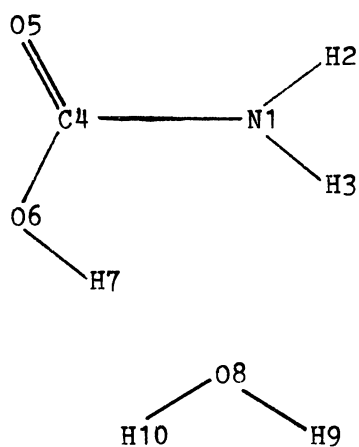


Bond Distance		Bond Angle	
N1-H2	.9897	H2-N1-H3	118.9297
N1-H3	.9886	C4-N1-H2	117.9464
C4-N1	1.3597	C4-N1-H3	123.1239
C4-O5	1.2101	N1-C4-O5	123.1689
C4-O6	1.3402	N1-C4-O6	114.9891
O7-H7	.9628	O5-C4-O6	121.8420
H7-O8	1.7670	C4-O6-H7	118.3921
O8-H9	.9001	O6-H7-O8	171.3676
O8-H10	.9516	H7-O8-H9	140.8256
		H9-O8-H10	111.9699
		H7-O8-H10	107.2045

UNITS = Angstroms and Degrees

TABLE XIII

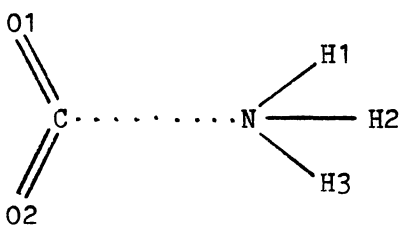
ATOMIC CHARGES ON MONO-HYDRATE OF  
CIS-CARBAMIC ACID



Atom	Charge
N1	-0.93
H2	+0.39
H3	+0.37
C4	+1.06
O5	-0.63
O6	-0.90
H7	+0.30
O8	-0.84
H9	+0.44
H10	+0.44

TABLE XIV

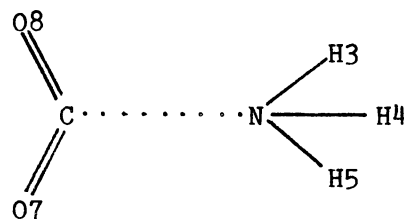
HF/4-31G OPTIMIZED GEOMETRY OF THE  
 $\text{CO}_2\text{-NH}_3$  LEWIS ADDUCT



Bond Distance		Bond Angle		Dihedral Angle	
O1-C	1.1588	O1-C -O2	174.8725	H1-N-C-O1	90.050
O2-C	1.1588	O1-C -N	92.5631		
C -N	2.7914	O2-C -N	92.5640		
H1-N	.9949	H1-N -H2	113.4874		
H2-N	.9951	H2-N -H3	113.4869		
H3-N	.9949	H3-N -H1	121.8420		

UNITS = Angstroms and Degrees

TABLE XV

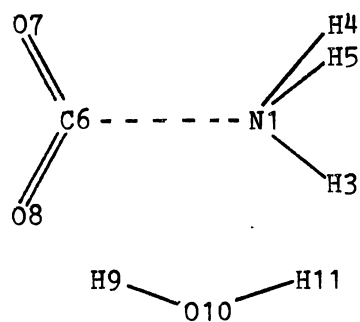
GEOMETRY OF CO<sub>2</sub>-NH<sub>3</sub> LEWIS ADDUCT VS. C-N INTERATOMIC DISTANCE

C-N	2.5	2.6	2.7	2.8	2.9	3.0	3.1	5.0	10.0
N-H3	.9963	.9958	.9953	.9949	.9946	.9943	.9941	.9901	.9912
N-H4	.9967	.9961	.9956	.9951	.9947	.9944	.9941	.9902	.9912
N-H5	.9963	.9958	.9953	.9949	.9946	.9943	.9941	.9902	.9912
C-O7	1.1612	1.1600	1.1593	1.1588	1.1584	1.1582	1.1581	1.1577	1.1577
C-O8	1.1612	1.1601	1.1593	1.1588	1.1584	1.1582	1.1581	1.1577	1.1577
H3-N -H4	112.5063	112.8491	113.1763	113.4388	113.7621	113.9871	114.1767	116.6346	115.8443
H3-N -H5	113.3577	113.6043	113.8365	114.0384	114.2373	114.3819	114.4979	116.8405	115.8478
H4-N -H5	112.5245	112.8669	113.1874	113.4486	113.7431	113.9527	114.1263	116.6754	115.8401
H3-N -C	105.6257	105.0264	104.0090	103.9061	103.4329	103.0448	102.7232	67.2202	65.3213
H4-N -C	106.4443	106.5360	106.6107	106.8094	106.7210	106.7498	106.7646	106.5691	107.0001
H5-N -C	105.6255	105.0374	104.9223	103.9392	103.4830	103.1071	102.7972	67.2590	65.3233
N -C -O8	94.7166	93.8100	93.0905	92.5616	92.0925	91.7576	91.4988	89.9452	89.9780
N -C -O8	94.7104	93.8020	93.0801	92.5461	92.0786	91.7424	91.4826	89.9410	89.9780
O7-C -O8	170.5729	172.3877	173.8288	174.8914	175.8278	176.4988	177.0174	179.8832	179.9552
O8-C-N-H3	29.7955	29.9098	29.8026	30.1329	30.2289	21.1275	30.3700	22.4864	21.1810

UNITS = Angstroms and Degrees

TABLE XVI

NON-OPTIMIZED GEOMETRY OF THE MONO-HYDRATE OF THE  
 $\text{CO}_2\text{-NH}_3$  LEWIS ADDUCT



Bond Distance		Bond Angle		Dihedral Angle	
N1-H3	.9963	H3-N1-H4	113.2836	H3-N1-C6-O7	146.5984
N1-H4	.9962	H3-N1-H5	113.4084	H3-N1-C6-O8	31.7718
N1-H5	.9959	H4-N1-H5	112.8734	N1-C6-O8-H9	21.7697
C6-N	2.7810	H3-N1-C6	107.5189	C6-O8-H9-O10	-177.8918
C6-O7	1.1549	H4-N1-C6	109.1601	C6-N1-H3-H11	- 71.1443
C6-O8	1.1615	H5-N1-C6	99.4785	H3-H11-O10-H9	- 38.3007
O8-H9	1.8888	N1-C6-O7	93.4565		
H9-O10	.9544	N1-C6-O8	90.8102		
O10-H11	.9490	O7-C6-O8	175.4330		
H11-H3	2.8920	C6-O8-H9	135.2999		
		O8-H9-O10	168.8626		

UNITS = Angstroms and Degrees



TABLE XVII

CONVERGENCE DATA FOR THE LAST POINT OF THE HF/4-31G  
OPTIMIZATION OF THE MONO-HYDRATE OF THE  
 $\text{CO}_2\text{-NH}_3$  LEWIS ADDUCT

Item	Value	Threshold	Converged
Maximum Force	.004278	.000450	NO
RMS Force	.001381	.000300	NO
Maximum Displacement	.002315	.001800	NO
RMS Displacement	.000817	.001200	YES

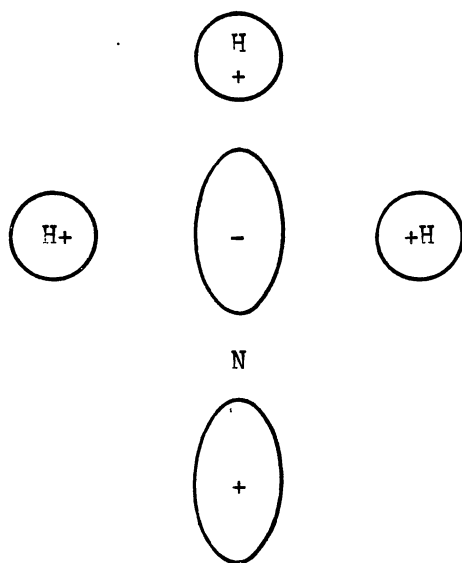


Figure 6. HOMO of Ammonia

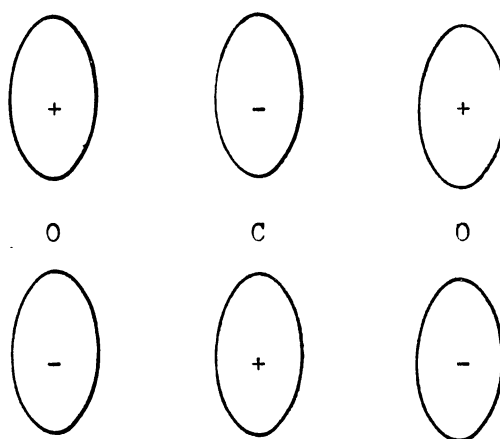


Figure 7. LUMO of Carbon Dioxide

TABLE XVIII

ATOMIC CHARGES ON ATOMS IN AMMONIA AND CARBON DIOXIDE VS.  
C-N INTERATOMIC DISTANCE

C-N	Charges						
	O	C	O	N	H	H	H
2.5	-0.52	+1.02	-0.52	-0.98	+0.34	+0.33	+0.34
2.6	-0.52	+1.01	-0.52	-0.98	+0.33	+0.33	+0.33
2.7	-0.51	+1.00	-0.51	-0.97	+0.33	+0.33	+0.33
2.7914	-0.51	+1.00	-0.51	-0.97	+0.33	+0.33	+0.33
2.8	-0.51	+1.00	-0.51	-0.97	+0.33	+0.33	+0.33
2.9	-0.50	+0.99	-0.50	-0.97	+0.33	+0.33	+0.33
3.0	-0.50	+0.99	-0.50	-0.97	+0.33	+0.33	+0.33
3.1	-0.50	+0.99	-0.50	-0.97	+0.33	+0.33	+0.33
5.0	-0.48	+0.97	-0.48	-0.97	+0.33	+0.33	+0.33
10.0	-0.48	+0.96	-0.48	-0.96	+0.32	+0.32	+0.32
Infinity	-0.45	+0.90	-0.45	-0.96	+0.32	+0.32	+0.32

ammonia is  $.90 - (-.96) = 1.86$ , which indicates a significant electrostatic attraction. In Table XIX, the eigenvalue and eigenvector of the HOMO of  $\text{H}_3\text{N}\dots\text{CO}_2$  are given as a function of C-N interatomic distance. The atomic orbitals of interest are the  $P_z$  orbitals of carbon and nitrogen. Upon examination of the  $P_z$  coefficients of the eigenvector of the HOMO as the C-N interatomic distance is decreased toward the optimum (2.7914Å), it is observed that the coefficients for  $\text{N}(P_z)$  decrease and the coefficients for  $\text{C}(P_z)$  increase. This indicates that as the C-N distance decreases, the HOMO involves more mixing of these  $P_z$  orbitals. Another indication of the interaction between carbon dioxide and ammonia as the C-N distance decreases is the shift in the O-C-O bond angle from linear to bent. At infinite separation, the O-C-O bond angle is 180 degrees due to the pi-bonding between carbon and the oxygens. As the C-N distance decreases, the bond angles about carbon shift toward 120 degrees, which is associated with  $sp^2$  atomic orbital hybridization. This suggests that the  $P_z$  orbital pi-bonding of the C-O double bond becomes less important as the C-N HOMO-LUMO interaction increases. Through examination of the atomic charges in the Lewis adduct vs. C-N interatomic distance (see Table XVIII), it is evident that as the C-N distance decreases, the hydrogens develop a more positive charge and the oxygens develop a more negative charge. The electron density shifts from the hydrogens to to nitrogen and from carbon to the oxygens. One of the hydrogens also becomes non-equivalent to the other two. The oxygens are equivalent as the C-N interatomic distance decreases from 10Å to the optimized value (2.7914Å). Calculations fixing the O-C-N-H dihedral angle to 90 degrees show the odd hydrogen to be at 90 degrees and to have a longer

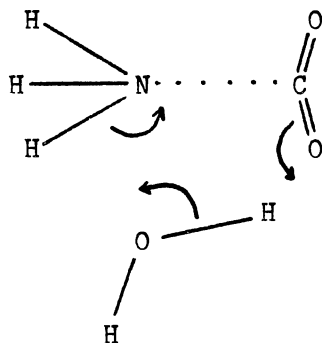
TABLE XIX

EIGENVALUE AND EIGENVECTOR OF HOMO OF  $\text{CO}_2\text{-NH}_3$  LEWIS  
ADDUCT VS. C-N INTERATOMIC DISTANCE

C-N(A)	2.7914	3.1000	5.0000	10.0000
E(AU)	-0.41938	-0.41202	-0.39143	-0.39086
N 1s	-0.04431	-0.05224	-0.03319	-0.03710
2s	0.27564	0.25882	0.19826	0.22233
2Px	-0.01198	-0.01130	0.00014	0.00003
2Py	-0.00775	-0.00795	-0.00074	0.00005
2Pz	-1.09280	-1.10061	-1.12459	-1.11850
H 1s	-0.06324	-0.06013	-0.04089	-0.04651
H 1s	-0.06323	-0.05661	-0.04048	-0.04647
H 1s	-0.06869	-0.06006	-0.04092	-0.04651
C 1s	0.00317	0.00064	0.00005	0.00000
2s	0.04409	0.04753	0.00348	0.00000
2Px	-0.00096	0.00029	0.00046	0.00000
2Py	0.00060	0.00070	0.00080	0.00000
2pz	-0.04473	-0.01902	-0.00165	0.00000
O 1s	0.00402	0.00283	-0.00007	0.00000
2s	-0.03750	-0.03157	-0.00161	0.00000
2Px	-0.02348	-0.02350	0.00061	0.00000
2Py	0.03810	0.01671	-0.00146	0.00000
2Pz	-0.10520	0.06436	0.00176	0.00000
O 1s	0.00402	0.00283	-0.00007	0.00000
2s	-0.03804	-0.03156	0.00161	0.00000
2Px	0.01766	0.02573	-0.00158	0.00000
2Py	0.03308	-0.01171	-0.00021	0.00000
2Pz	-0.10695	-0.06463	0.00176	0.00000

N-H bond distance.

When a water molecule is included with the Lewis adduct, the C-O bond distances and charges become non-equivalent. The oxygen nearest to the hydrogen of water is more electronegative and has a longer C-O bond length than the other, which is consistent with the structure obtained for carbamic acid. This suggests the possibility that in aqueous solution the formation of carbamic acid can occur through the transfer of  $H^+$  from water by a mechanism such as:



In the search for the optimized (minimum energy) structure of  $H_3N...CO_2$ , the Lewis adduct, a negative eigenvalue was obtained, which indicates that a saddle point is present. Optimization calculations for the Lewis adduct were made using the Gaussian 82 command options, `OPT=(TIGHT,CALL,NOEIGENTEST)`. These options call for lower tolerances for convergence, analytically calculated second derivatives with respect to the energy and no testing for negative eigenvalues. The negative eigenvalue corresponds to the imaginary frequency obtained. The imaginary frequency is a rotation about the C-N axis as shown in Figure 8. The structure obtained for the Lewis adduct is optimum since there is apparently little or no rotational barrier at

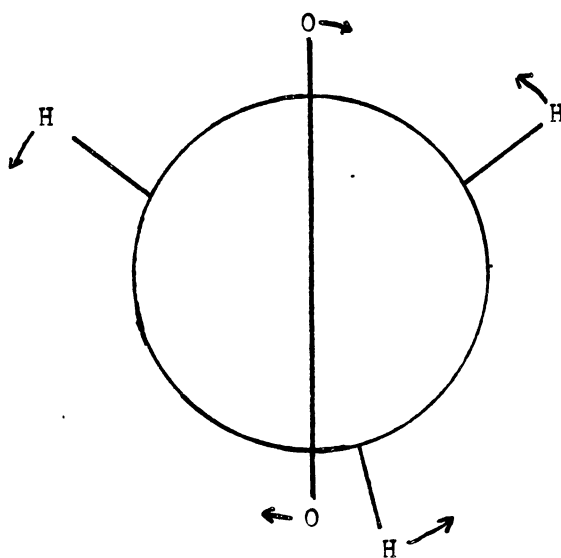


Figure 8. Vibrational Eigenvector  
Obtained for the  
 $\text{CO}_2\text{-NH}_3$  Lewis Adduct

this level of computation (see energy calculations).

The HF/6-31G\* optimized geometry obtained for the Lewis adduct agrees with that obtained by Amos et al. (see Figure 5, p. 18) (30). This geometry was the best in an optimization for the Lewis adduct with the command line OPT=(TIGHT,NOEIGENTEST). At this point the convergence criterion for the TIGHT option was not met, but the values were well below the tolerances of an ordinary optimization run. When this geometry was used for a frequency analysis run, which utilizes analytically calculated second derivatives with respect to the energy, it was determined not to be convergent. The frequency analysis for the Lewis adduct at the 6-31G\* level produces a negative eigenvalue and an imaginary frequency. The imaginary frequency is a rotation about the C-N axis just as that obtained at the 4-31G level.

The planar geometry of CIS and TRANS-carbamic acid as shown in Tables IX and X is very interesting. Nitrogen compounds in which lone pair electrons are present on nitrogen are predicted to be pyramidal in shape by the VSEPR model. Carbamic acid does not display this pyramidal geometry. One explanation for this behavior is the presence of the electropositive carbon adjacent to the nitrogen. The atomic charges in CIS and TRANS-carbamic acid are given in Table XI. Values in Table XI show the difference in charge between carbon and nitrogen to be  $1.07 - (-.93) = 2.00$  and  $1.03 - (-.90) = 1.93$  for CIS and TRANS-carbamic acid, respectively. An electropositive atom tends to withdraw electron density from neighboring electron rich areas. The HOMO's of CIS and TRANS-carbamic acid are pictorially presented in Figures 9 and 10, respectively. The HOMO's of both CIS and TRANS-



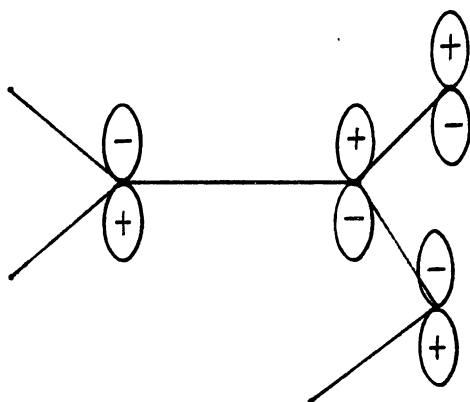
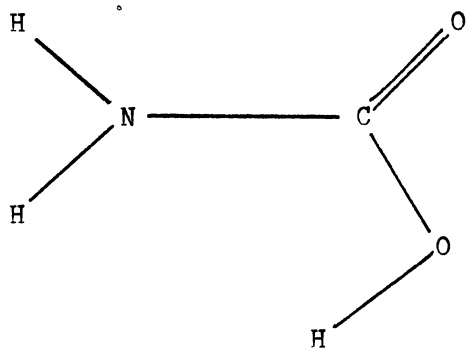


Figure 9. HOMO of CIS-Carbamic Acid

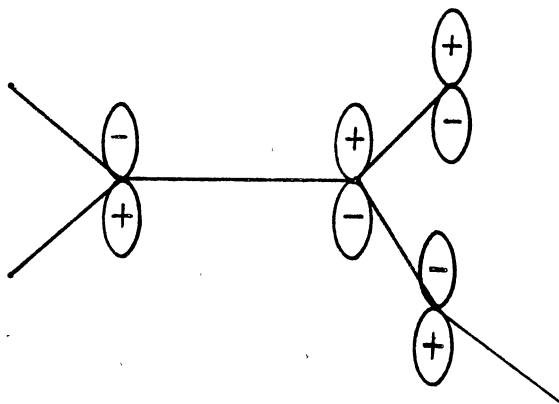
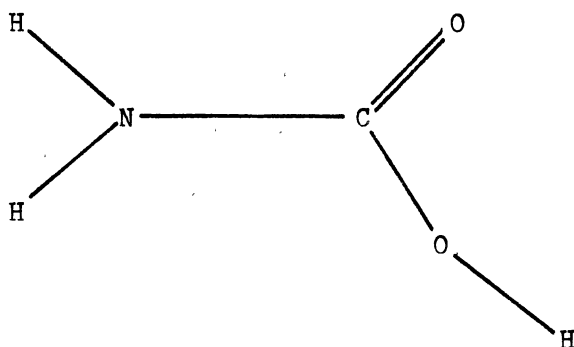


Figure 10. HOMO of TRANS-Carbamic Acid

carbamic acid are non-bonding between carbon and both nitrogen and the OH oxygen and in pi-bonding between carbon and the carbonyl oxygen ( $C(P_y)-O(P_y)$ ). The  $N(P_y)$  orbital on nitrogen contains the lone pair of electrons. By the VSEPR model, the spatial requirements of a lone pair of electrons is greater than that of bonding electrons due to the more diffuse nature of a lone pair orbital. If electron density of a lone pair orbital is decreased, the orbital will be less diffuse and therefore will require less space. Without the effects of the lone pair orbital on the geometry about nitrogen, the bond angles will be 120 degrees, which are the calculated angles.

TRANS-carbamic acid was determined to be the lower energy isomer of carbamic acid by Pople et al. (31) and Schafer et al. (33). This current study has likewise determined TRANS-carbamic acid to be the lower energy isomer. The total energies of CIS and TRANS-carbamic acid obtained in this study are lower than those obtained by Pople et al. This was expected since Pople's group used "standard" bond distances and bond lengths while full geometry optimizations were performed in this study.

#### Energy Calculations

The HF/4-31G and MPk/4-31G//HF/4-31G,  $k=2,3,4$  energies for  $H_2$ ,  $N_2$ ,  $O_2$ ,  $C(g)$ ,  $H_2O$ ,  $NH_3$ ,  $CO_2$ ,  $H_3N...CO_2$ , CIS and TRANS-carbamic acid and  $H_2O.CIS-V_2NCO_2H$  are given in Table XX. In Table XXI, the HF/4-31G and MPk/4-31G//HF/4-31G,  $k=2,3,4$  energies of  $H_3N...CO_2$ , the Lewis adduct are presented as a function of C-N interatomic distance. The MP4SDQ energies of the Lewis adduct are plotted as a function of the C-N interatomic distance in Figure 11. Through the examination of Figure

TABLE XX

## TOTAL ENERGIES OF MOLECULES OF INTEREST

Chemical Species	Total Energy (Kcal/mol)				
	HF	MP2	MP3	MP4SDQ	ZPE(HF)
H <sub>2</sub>	- 707.10	- 717.93	- 721.16	- 722.15	6.65
N <sub>2</sub>	- 68244.36	- 68391.35	- 68377.63	- 68386.53	3.82
O <sub>2</sub>	- 93745.58	- 93894.92	- 93885.27	- 93892.79	2.47
C(1)	- 23559.59	-23583.18	- 23591.56	- 23594.80	- - -
H <sub>2</sub> O	- 47633.43	- 47713.34	- 47714.51	- 47717.03	14.03
NH <sub>3</sub>	- 35207.51	- 35278.98	- 35283.58	- 35285.86	22.78
CO <sub>2</sub>	-117550.18	-117771.44	-117750.39	-117765.12	7.31
H <sub>3</sub> N...CO <sub>2</sub>	-152762.98	-153055.38	-153039.71	-153056.45	31.58
TRANS-H <sub>2</sub> NCO <sub>2</sub> H	-152774.26	-153049.33	-153044.98	-153055.73	35.23
CIS-H <sub>2</sub> NCO <sub>2</sub> H	-152763.05	-153038.73	-153034.41	-153045.20	34.34
CIS-H <sub>2</sub> NCO <sub>2</sub> H.H <sub>2</sub> O	-200409.59	-200765.33	-200761.93	-200775.17	- - -

TABLE XXI

TOTAL ENERGY OF THE CO<sub>2</sub>-NH<sub>3</sub> LEWIS ADDUCT VS. C-N  
INTERATOMIC DISTANCE

C-N(Å)	Total Energy (Kcal/mol)			
	HF	MP2	MP3	MP4SDQ
2.5	-152762.05	-153054.36	-153039.08	-153055.63
2.6	-152762.62	-153054.94	-153039.51	-153056.14
2.7	-152762.091	-153055.26	-153039.70	-153056.39
2.7914	-152762.98	-153055.98	-153039.71	-153056.45
2.8	-152762.98	-153055.38	-153039.71	-153056.45
2.9	-152762.90	-153055.34	-153039.57	-153056.35
3.0	-152762.71	-153055.20	-153039.34	-153056.16
3.1	-152762.44	-153054.99	-153039.04	-153055.90
5.0	-152757.69	- - - -	- - - -	- - - -
10.0	-152757.68	- - - -	- - - -	- - - -
Infinity	-152757.69	-153050.42	-153033.97	-153050.98

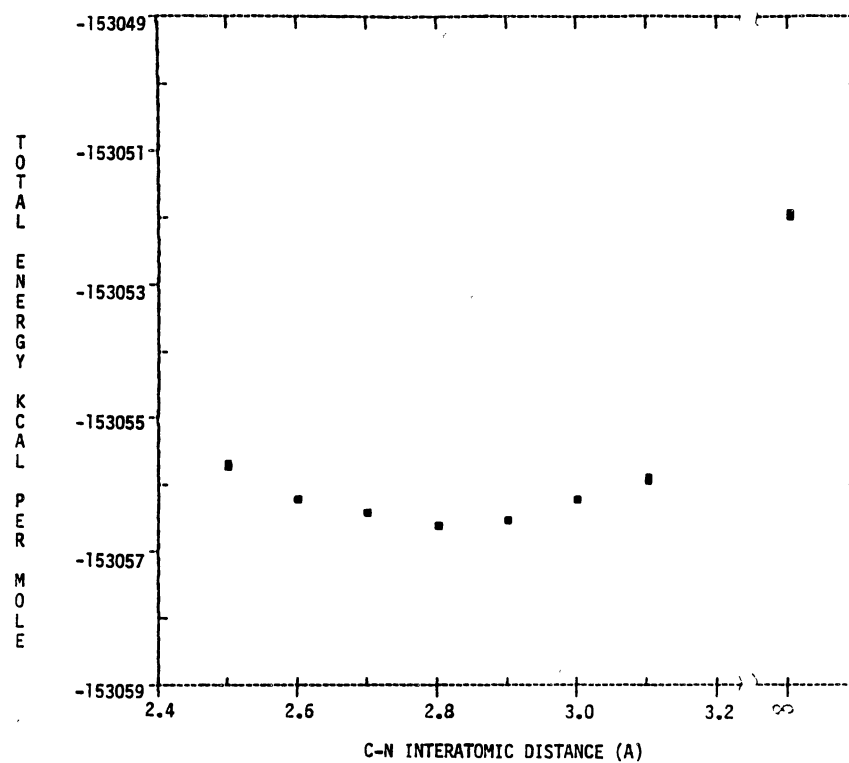


Figure 11. Plot of Total Energy (MP4SDQ) vs. C-N Interatomic Distance of the  $\text{CO}_2\text{-NH}_3$  Lewis Adduct

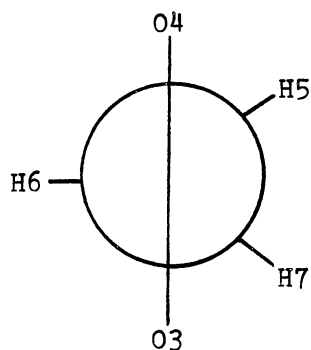
11 and Table XXI it is apparent that the formation of a  $\text{H}_3\text{N}...\text{CO}_2$  Lewis adduct is energetically favored by 5.47 Kcal/mol at the MP4SDQ/4-31G//HF/4-31G level and that the well in this area of the potential energy surface is quite shallow.

The energies calculated by variational methods provide an upper limit to the true energy. Moller-Plesset theory is not a variational method but previous calculations have shown it to reliably predict correlation energy in a faster time and at lower cost than CI methods. The calculated energy depends on the quality of the basis set used and the degree of electron correlation employed by the calculation. Energies of atomization calculated at the MP4SDQ/6-311G\*/HF/6-311G\* level predict electronic energies to within 2 Kcal/mol of the experimental value (49). Calculations at the MP4SDQ/4-31G//HF/4-31G level are expected to predict electronic energies to within approximately 10-15 Kcal/mol (see Table XXIV, p. 51).

The HF, MP2, MP3 and MP4SDQ total electronic energy was calculated as a function of the O-C-N-H dihedral angle of the Lewis adduct. The geometry and energy results for these calculations are shown in Table XXII. The greatest energy difference calculated at the MP4SDQ/4-31G//HF/4-31G level was .01 Kcal/mol. This is below the uncertainty in energy measurements for the Gaussian 82 program. These results indicate that there is no rotational energy barrier about the C-N axis in  $\text{H}_3\text{N}...\text{CO}_2$ , the Lewis adduct. Klemperer et al.(28) estimate the rotational barrier in the Lewis adduct to be approximately .014 Kcal/mol. Since this is well below RT at 298°K (.592 Kcal/mol), there is free rotation between the  $\text{NH}_3$  and  $\text{CO}_2$  subgroups at this temperature.

TABLE XXII

GEOMETRY AND TOTAL ENERGY OF THE  $\text{CO}_2\text{-NH}_3$  LEWIS ADDUCT VS.  
O-C-N-H DIHEDRAL ANGLE<sup>3</sup>



H4-N-C-O4	0.	10.	20.	29.95
C-O3	1.1590	1.1589	1.1589	1.1588
C-O4	1.1587	1.1588	1.1588	1.1588
C-N	2.7914	2.2707	2.7913	2.7916
N-H5	.9949	.9948	.9948	.9949
N-H6	.9950	.9950	.9949	.9951
N-H7	.9951	.9951	.9952	.9949
O3-C-O4	174.8706	174.8723	174.8755	174.8725
O3-C-N	92.1452	92.2308	92.1763	92.5631
O4-C-N	92.9841	92.8965	92.9479	92.5640
H5-N-C	105.6498	105.4203	105.5104	104.1985
H6-N-C	103.1738	103.5627	103.3843	106.1235
H7-N-C	105.7703	105.5519	105.6399	104.2007
H5-N-H6	113.2684	113.9491	114.0759	113.4874
H6-N-H7	113.2684	113.2913	113.4103	113.4869
H7-N-H5	113.8404	113.7745	113.5339	114.0607
E(HF)	-152762.98	-152762.97	-152762.97	-152762.98
E(MP2)	-153055.38	-153055.37	-153055.37	-153055.38
E(MP3)	-153039.71	-153039.70	-153039.70	-153039.71
E(MP4SDQ)	-153056.45	-153056.44	-153056.44	-153056.44
ZPE	31.58	- - -	- - -	31.58

UNITS = ANGSTROMS, DEGREES AND Kcal/mol



During the vibrational frequency analysis portion of the Gaussian 82 program, zero point energies, thermal energies and entropies are also predicted. The results of these calculations for the chemical species studied appear in Table XXIII. From the above data, a number of thermodynamic quantities may be calculated. Enthalpies of formation may be calculated using the formula

$$\Delta H^{\circ}(298) = \Delta \text{MP4SDQ} + \Delta \text{ZPE} + \Delta \text{Thermal Energy (298)}$$

where the differences in energies are those between the molecule and the elements from which it is composed in their standard states. The Gibb's free energies and equilibrium constants in the gas phase may be calculated using

$$\Delta G^{\circ} = \Delta H^{\circ} - T \Delta S^{\circ}$$

and

$$K_p^{\circ} = \exp (-\Delta G^{\circ}/RT)$$

Enthalpies of formation calculated for all molecules studied are shown in Table XXIV. In comparison to experimental values, the calculated enthalpies of formation do compare well with measured values. Thermodynamic quantities for the reactions of interest to this study may be calculated from formation data using the relation

$$\Delta X^{\circ} = \sum_{\text{prod.}} v_i X_i^{\circ} - \sum_{\text{react.}} v_i X_i^{\circ}$$

where  $X = H, G$  or  $S$  and  $v_i$  are the stoichiometric coefficients. The reactions of interest are

TABLE XXIII

CALCULATED ZERO POINT ENERGIES, THERMAL ENERGIES AND  
ENTROPIES FOR MOLECULES OF INTEREST

Chemical Species**	MP4SDQ (Kcal/mol)	ZPE (Kcal/mol)	Thermal (Kcal/mol)	S°(calc) (cal/mol K)	S°(exp)*
H2	- 722.15	6.65	1.48	31.062	31.208
N2	- 68386.53	3.83	1.48	45.710	45.770
O2	- 93892.82	2.48	1.48	48.948	49.003
C(1)	- 23594.80	0.00	.89	- - -	37.760
H2O	- 47717.03	14.03	1.77	44.947	45.104
NH3	- 35285.86	22.78	1.88	46.153	45.970
CO2	-117765.12	7.31	1.66	51.110	- - -
H3N...CO2	-153056.45	31.58	3.58	73.087	- - -
TRANS-H2NCO2H	-153055.73	35.23	2.36	64.418	- - -
CIS-H2NCO2H	-153045.20	34.34	2.67	66.677	- - -
CIS-H2NCO2H.H2O	-200775.17	- - -	- - -	- - -	- - -

\*From Ref. 44

\*\*All chemical species are in the gas phase.

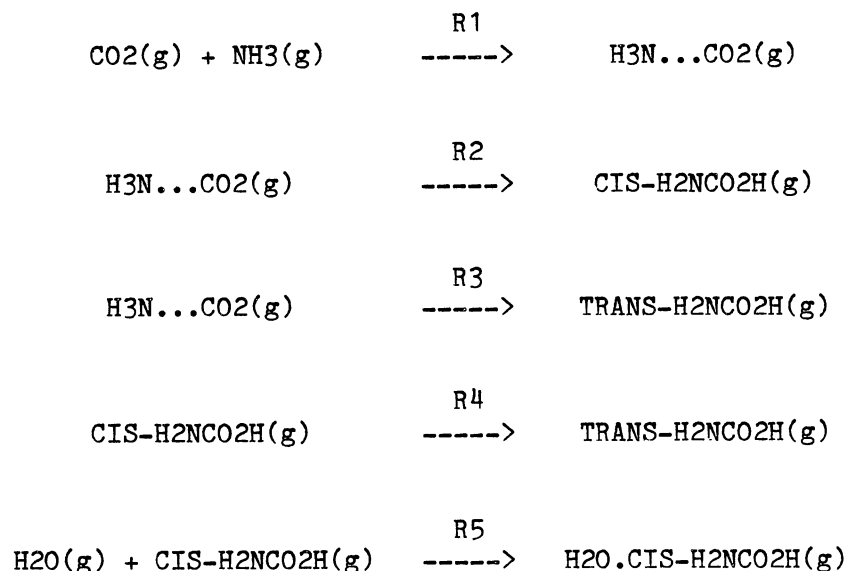
TABLE XXIV

## CALCULATED FORMATION THERMOCHEMICAL DATA

Chemical Species	Kcal/mol					cal/mol K	
	Calc.	Calc.	Exp.	Calc	Exp.	Calc.	Exp.
	H°(298)	$\Delta H_f^\circ(298)$	$\Delta H_f^\circ(298)$	$\Delta G_f^\circ(298)$	$\Delta G_f^\circ(298)$	$\Delta S_f^\circ(298)$	$\Delta S_f^\circ(298)$
H2(g)	- 714.02	+ 0.0	+ 0.0	+ 0.0	+ 0.0	+ 0.0	+ 0.0
N2(g)	- 68381.22	+ 0.0	+ 0.0	+ 0.0	+ 0.0	+ 0.0	+ 0.0
O2(g)	- 93888.86	+ 0.0	+ 0.0	+ 0.0	+ 0.0	+ 0.0	+ 0.0
C(g)	- 23592.41	- - -	+171.28	- - -	+160.43	- - -	+36.39
H2O(g)	- 47701.23	- 42.78	- 57.79	- 39.62	- 54.63	-10.589	-10.61
CO2(g)*	-117756.15	-103.60	- 94.06	-103.30	- 94.26	+ 0.792	+ 0.685
NH3(g)	- 35261.20	+ 0.44	- 11.01	+ 7.39	- 3.94	-23.295	-23.73
O2C...NH3(g)*	-153021.29	-107.10	- - -	- 93.18	- - -	-46.679	- - -
TRANS-H2NCO2H(g)*	-153018.14	-103.95	- - -	- 87.45	- - -	-55.348	- - -
CIS-H2NCO2H(g)*	-153008.19	- 94.00	- - -	- 78.17	- - -	-53.089	- - -

\* Formation data is corrected based on the experimental formation data for C(g).

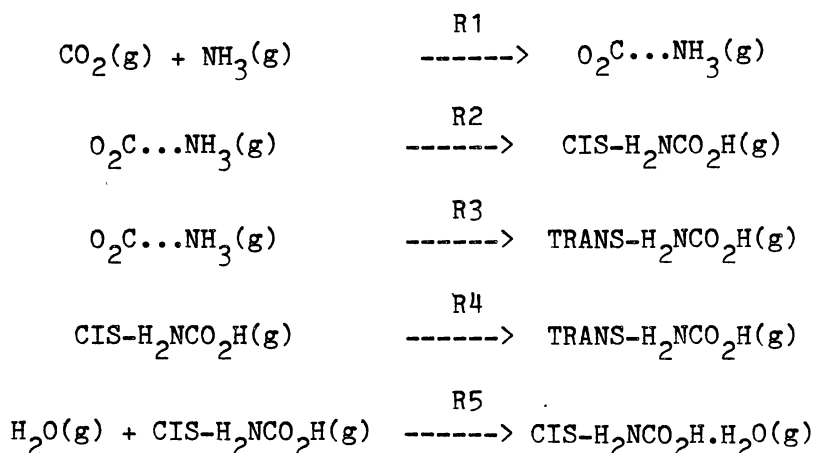
\*\* Experimental data is from reference 44.



Results for energy differences and thermodynamic quantities for these reactions are given in Table XXV.

The uncertainties in  $\Delta H^\circ_{\text{rxn}}$ ,  $\Delta S^\circ_{\text{rxn}}$  and  $\Delta G^\circ_{\text{rxn}}$  can be estimated through examination of the errors in formation data. The enthalpies of formation can be high by as much as 10-15 Kcal/mol. Since they are always in error on the high side, little propagation of error is likely to occur when differences are taken. Thus the estimated error in the enthalpies of reaction is 10-15 Kcal/mol. The entropies of reaction, by the same kind of argument, may be in error up to 2 cal/(mol K). Since Gibb's free energies were calculated using enthalpy and entropy data, the error in the Gibb's free energy will be a result of the combined errors in the enthalpies and entropies. At 298°K, the error in  $T\Delta S^\circ$  is less than 1 Kcal/mol. This leads to an approximate error in  $\Delta G^\circ_f$  equal to the error in  $\Delta H^\circ_f$ . At the MP4SDQ/4-31G//HF/4-31G level of approximation and at 298°K, reaction R1, the formation of the Lewis adduct is energetically favored but is not spontaneous due to the

TABLE XXV

CALCULATED ENERGY AND THERMOCHEMICAL DATA FOR  
REACTIONS OF INTEREST

	R1	R2	R3	R4	R5
<hr/>					
Kcal/mol					
<hr/>					
$\Delta\text{HF}/4\text{-}31\text{G}$	- 5.29	- 0.07	-11.28	-11.21	-13.11
$\Delta\text{HF}/6\text{-}31\text{G}^*$	- 5.43	- - -	- - -	- - -	-13.26
$\Delta\text{MP2}/4\text{-}31\text{G}/\text{HF}/4\text{-}31\text{G}$	- 4.95	+16.65	+ 6.05	-10.60	-13.01
$\Delta\text{MP3}/4\text{-}31\text{G}/\text{HF}/4\text{-}31\text{G}$	- 5.74	+ 5.30	- 5.27	-10.57	-12.94
$\Delta\text{MP4SDQ}/4\text{-}31\text{G}/\text{HF}/4\text{-}31\text{G}$	- 5.47	+11.25	- 0.72	-10.53	- - -
$\Delta\text{ZPE}$	+ 1.49	+ 2.76	+ 3.65	+ 0.89	- - -
$\Delta(\text{MP4SDQ} + \text{ZPE})$	- 3.98	+14.01	+ 2.93	- 9.64	- - -
$\Delta\text{H}^\circ(298)$	- 3.94	+13.10	+ 3.15	- 9.95	- - -
$\Delta\text{G}^\circ(298)$	+ 2.73	+15.01	+ 5.73	- 9.28	- - -
<hr/>					
cal/mol K					
<hr/>					
$\Delta\text{S}^\circ(298)$	-24.176	- 6.410	- 8.669	- 2.259	- - -
$\ln K^\circ$	- 4.6	-25.34	- 9.67	+15.66	- - -
<hr/>					

positive  $\Delta G_{\text{rxn}}^\circ$  (298) value. Reactions R2 and R3, the formation of carbamic acid from the Lewis adduct are not energetically favored nor are they spontaneous. Reaction R4, the CIS to TRANS conversion of carbamic acid is both energetically favored and spontaneous. Ignoring other reactions, these results indicate that at 298°K in the gas phase, a 1:1 mixture of carbon dioxide and ammonia will exist primarily as free NH<sub>3</sub> and CO<sub>2</sub> and neither the Lewis adduct nor carbamic acid will form. With initial CO<sub>2</sub> and NH<sub>3</sub> partial pressures of 1 atm, the  $\ln K_p^\circ$  calculated for reaction R1 indicates that the equilibrium partial pressure of the Lewis adduct is 7.6 mm Hg. This quantity is detectable but has not been experimentally observed. Perhaps the Lewis adduct is not found experimentally due to kinetic factors involved in the forward reaction of R1. Reaction R5, the monohydration of CIS-carbamic acid is energetically favored at the MP4SDQ/4-31G//HF/4-31G level.

#### Vibrational Frequency Calculations

Vibrational frequencies for the molecules investigated are given in Tables XXVI thru XXIX. The results of 6-31G\* frequency calculations are given, but they are not completely reliable since the geometry was determined not to be stationary. According to Pople et al. (42), the results of vibrational frequency calculations using split valence double zeta basis sets such as 4-31G and 6-31G\* are too large by approximately 10-15%. This holds true for most cases where experimental values are available. The major deviations from deviations from experimental measurements appear below 1000cm<sup>-1</sup>. Infrared spectra of a 1:1 mixture of CO<sub>2</sub> and NH<sub>3</sub> were not available for comparison with the calculated values for the Lewis adduct.

TABLE XXVI

VIBRATIONAL FREQUENCIES OF  $H_2$ ,  $N_2$ ,  $O_2$ ,  $H_2O$ ,  $CO_2$  AND  $NH_3$ 

Assignment	Frequency ( $cm^{-1}$ )			Reference
	4-31G	6-31G*	Experimental	
$H_2$ (SIG)	4649	- - -	4395	47
$N_2$ (SIG)	2675	- - -	2360	47
$O_2$ (SIG)	1731	- - -	1580	47
$H_2O$ (a1)	3958	4070	3657	42
(a1)	1743	1826	1595	42
(b2)	4110	4188	3756	42
$CO_2$ (SIG)	1420	- - -	1388	47
(PIU)	644	- - -	667	47
(SIU)	2404	- - -	2349	47
$NH_3$ (a1)	3760	3690	3337	42
(a1)	621	1207	950	42
(e)	3957	3823	3444	42
(e)	1821	1849	1627	42

TABLE XXVII

## CALCULATED VIBRATIONAL FREQUENCIES OF CIS-CARBAMIC ACID

Frequency ( $\text{cm}^{-1}$ )		Assignment
Calculated HF/4-31G	Corrected* HF/4-31G	
156	136	out of plane distortion
519	452	out of plane distortion
558	485	$\text{H}_2\text{N}-\text{CO}_2\text{H}$ in plane wobble
659	573	O-C-O bend
663	577	$\text{H}_2\text{N}-\text{CO}_2\text{H}$ out of plane bend
861	749	out of plane distortion
1019	887	$\text{H}_2\text{N}-\text{CO}_2\text{H}$ in plane bend
1168	1016	in plane distortion
1303	1131	in plane distortion
1488	1295	C-N stretch
1836	1597	H-N-H bend
1952	1698	H-N-C (carbonyl side) bend
3845	3315	H-N symmetric stretch
3974	3457	H-N asymmetric stretch
4020	3497	H-O stretch

\* Corrected = Calculated x .87 (see text)



TABLE XXVIII

## CALCULATED VIBRATIONAL FREQUENCIES OF TRANS-CARBAMIC ACID

Frequency (cm <sup>-1</sup> )		Assignment
Calculated HF/4-31G	Corrected* HF/4-31G	
535	465	in plane distortion
563	490	out of plane distortion
629	547	out of plane distortion
632	550	H <sub>2</sub> N-CO <sub>2</sub> H in plane wobble
658	572	out of plane distortion
879	765	out of plane distortion
1040	905	in plane distortion
1207	1050	H <sub>2</sub> N-CO <sub>2</sub> H in plane bend
1320	1148	in plane distortion
1594	1348	C-N stretch
1816	1580	H-N-H bend
1921	1671	H-N-C (carbonyl side) bend
3854	3353	H-N symmetric stretch
3990	3471	H-N asymmetric stretch
4005	3484	H-O stretch

\* Corrected = Calculated x .87 (see text)

TABLE XXIX

CALCULATED HF/4-31G AND HF/6-31G\* VIBRATIONAL FREQUENCIES  
OF THE CO<sub>2</sub>-NH<sub>3</sub> LEWIS ADDUCT

Frequency (cm <sup>-1</sup> )				
4-31G			6-31G*	
Lewis Adduct	CO <sub>2</sub>	NH <sub>3</sub>	Lewis Adduct	Assignment
- 7			- 1	C-N axis rotation
110(96)			74(64)	NH <sub>3</sub> wobble
133(116)			110(96)	C-N stretch
271(236)			185(161)	NH <sub>3</sub> wobble
336(292)			246(214)	NH <sub>3</sub> wobble
		621(540)		symmetric bend
632(541)			731(636)	mixed symmetric bend
	644(560)			bend
662(576)			756(658)	CO <sub>2</sub> bend
924(804)			1235(1074)	NH <sub>3</sub> symmetric bend
1415(1231)			1515(1318)	CO <sub>2</sub> symmetric stretch
	1420(1235)			symmetric stretch
		1821(1584)		asymmetric bend
1839(1600)			1847(1607)	NH <sub>3</sub> asymmetric bend
1840(1601)			1847(1607)	NH <sub>3</sub> asymmetric bend
2401(2089)			2580(2245)	CO <sub>2</sub> asymmetric stretch
	2404(2091)			asymmetric stretch
3723(3239)			3692(3212)	NH <sub>3</sub> symmetric stretch
		3760(3271)		symmetric stretch
3900(3393)			3822(3325)	NH <sub>3</sub> asymmetric stretch
3904(3396)			3825(3328)	NH <sub>3</sub> asymmetric stretch
		3957(3443)		asymmetric stretch

\*Values in parentheses are corrected by a factor of .87.

## CHAPTER IV

### SUMMARY AND CONCLUSIONS

The interaction of  $\text{CO}_2$  with  $\text{NH}_3$  is mainly due to the electrostatic attraction between the electronegative nitrogen of ammonia and the electropositive carbon of carbon dioxide. Carbon dioxide and ammonia undergo a Lewis type acid-base interaction to produce a weakly bound complex, the Lewis adduct.

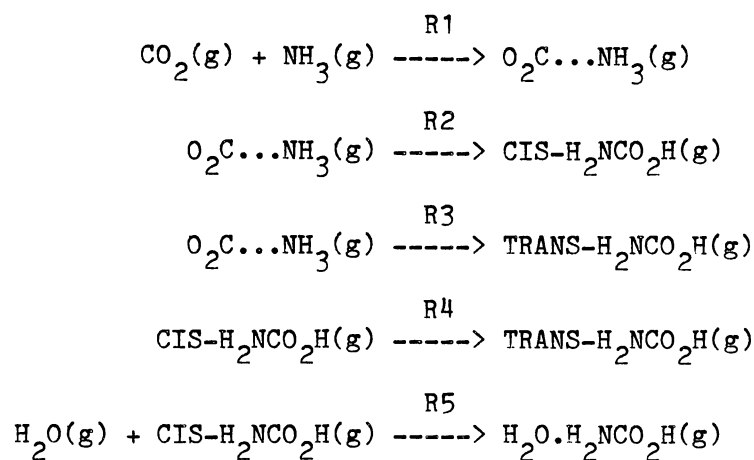
The rotational barrier about the C-N axis of the Lewis adduct has been calculated at the MP4/4-31G//HF/4-31G level to be less than 10 cal/mol. Since this is less than RT at normal temperature (592 cal/mol), free rotation is allowed between the  $\text{CO}_2$  and  $\text{NH}_3$  subgroups at 298 K.

Equilibrium geometries of  $\text{H}_2$ ,  $\text{N}_2$ ,  $\text{O}_2$ ,  $\text{H}_2\text{O}$ ,  $\text{CO}_2$ ,  $\text{NH}_3$ ,  $\text{O}_2\text{C}\cdots\text{NH}_3$ , CIS- $\text{H}_2\text{NCO}_2\text{H}$ , TRANS- $\text{H}_2\text{NCO}_2\text{H}$ , and  $\text{H}_2\text{O}\cdot\text{H}_2\text{NCO}_2\text{H}$  have been calculated at the HF/4-31G level. The geometry of  $\text{O}_2\text{C}\cdots\text{NH}_3$  has also been calculated at the HF/6-31G\* level. The C-N interatomic distance obtained at the HF/6-31G\* level (2.950Å) agrees well with the experimental value obtained by Klemperer et al. (2.9875Å) (29). The geometry of carbamic acid is planar. This may be due to withdrawal of electron density from the lone pair orbital of nitrogen. The lessening of electron density in the lone pair orbital of nitrogen decreases the electron repulsion and therefore lessens the spatial requirements of that orbital. This

allows the bonding orbitals to attain the 120 degree planar geometry.

TRANS-carbamic acid was found to be the lower energy form of carbamic acid. This agrees with the findings of Pople et al. (31) and Schafer et al. (33).

The thermochemical and energetic results for the reactions studied are summarized below:



Kcal/mol	R1	R2	R3	R4	R5
$\Delta\text{MP4SDQ}$	- 5.47	+11.25	-0.72	-10.53	-12.94
$\Delta\text{MP4SDQ} + \Delta\text{ZPE}$	- 3.98	+14.01	+2.93	- 9.64	- - -
$\Delta\text{G}^\circ_{\text{rxn}}(298)$	+ 2.73	+15.01	+5.73	- 9.28	- - -
$\Delta\text{H}^\circ_{\text{rxn}}(298)$	- 3.94	+13.10	+3.15	- 9.95	- - -
cal/mol					
$\Delta\text{S}^\circ_{\text{rxn}}(298)$	-24.18	- 6.41	-8.67	- 2.26	- - -
$\ln K_p^\circ$	- 4.60	-25.34	-9.67	+15.66	- - -

Reaction R1, the formation of the Lewis adduct, is exothermic and non-spontaneous. Reactions R2 and R3, the formation of CIS or TRANS-

carbamic acid from the Lewis adduct are endothermic and non-spontaneous. Reaction R4, the CIS to TRANS conversion of carbamic acid is exothermic and spontaneous. Reaction R4, the monohydration of CIS-carbamic acid is energetically favored.

In the anhydrous gas phase, the formation of carbamate, if it occurs, does not proceed through the formation of carbamic acid. These calculations indicate that in the anhydrous gas phase at 298°K, a 1:1 mixture of  $\text{NH}_3$  and  $\text{CO}_2$  will exist primarily as the non-associated gases and the Lewis adduct will be a minor component. In the presence of water, carbamate formation may occur through a proton transfer from water to one of the oxygens of the Lewis adduct, while the adduct loses a proton from nitrogen.

## BIBLIOGRAPHY

1. Beyer, A., Karphen, A. and Schuster, P., "Energy Surfaces of Hydrogen Bonded Complexes in the Vapor Phase", in Hydrogen Bonds, Schuster, P. (Ed.), Springer-Verlag, New York, New York (1984).
2. Leopold, K. R., Fraser, G. T. and Klemperer, W. J., J. Chem. Phys., 80, 1039 (1984).
3. Peterson, K. I. and Klemperer, W. J., J. Chem. Phys., 80, 2439 (1984).
4. Heylin, M. (Ed.), Chem. & Eng. News, 62(5) (1984).
5. Lemkowitz, S. M., Vet. E. and van den Berg, P. J., J. Appl. Chem. Biotechnol., 27(7), 335 (1977).
6. Maddox, R. N. and Mains, G. J., "Data and Design for Amine Treating", Presented at 63rd Annual GPA Convention March 19-21, 1984, New Orleans, LA.
7. Gmelin, L., HandBuch Anorgan. Chem., Berlin, Vol. 23, pp. 348-62 (1936).
8. Lishnevskii, V. A. and Madzievskaya, T. A., Russ. J. Phys. Chem., 56(9), 1342 (1982).
9. Briggs, T. R. and Migrdichian, V. A., J. Phys. Chem., 28, 1121 (1924).
10. Janjic, D., Helv. Chim. Acta, 47(7), 1879 (1964).
11. Bennett, R. N., Richie, P. D., Roxburgh, D. and Thomson, J., Trans. Faraday Soc., 49, 925 (1953).
12. Edgar, E. P. Jr., Potts, J. E. and Potts, G. D., Ind. Eng. Chem., 38, 454 (1946).
13. Fenton, H. J. H., Proc. Roy. Soc. (London), 39, 386 (1885).
14. Burrows, G. H. and Lewis, G. N., J. Am. Chem. Soc., 34, 993 (1912).
15. Christensson, F., Koefoed, H. C. S., Petersen, A. C. and Rasmussen, K., Acta Chem. Scand., A32, 15 (1978).

16. Faurholt, C., K. Dan. Vidensk. Selsk., Mat.-Fys. Medd., 3, 20 (1921).
17. Van Krevelan, D. W., Hoftijzer, P. J. and Huntjens, F. J., Recl. Trav. Chim. Pays-Bas., 68, 191 (1949).
18. Edwards, T. J., Newman, J. and Prausnitz, J. M., AIChE J., 21(2), 248 (1975).
19. Beutier, D. and Renon, H., Ind. Eng. Chem. Process Des. Dev., 17(3), 220 (1978).
20. Yoshida, T., Proc. Imp. Acad. (Tokyo), 12, 191 (1936).
21. Faurholt, C., Z. Anorg. Allegem. Chem., 120, 85 (1921).
22. Kucheryavyi, V. I., Gal'perin, V. A., Moncharzh, E. M. and Finkel'shtein, A. I., Zh. Prikl. Khim., 47(3), 529 (1974).
23. Fawsitt, C. E., Z. Phys. Chem., 41, 602 (1902).
24. Pinsent, B. R. W., Pearson, L. and Roughton, F. J. W., Trans. Faraday Soc., 52, 1594 (1956).
25. Baranski, A., Chemia Stosowana, 7(2), 231 (1963).
26. Frasco, D., J. Chem. Phys., 41(7), 2134 (1974).
27. Hisatsune, I. C., Can. J. Chem., 62, 945 (1984).
28. Fraser, G. T., Leopold, K. R. and Klemperer, W., J. Chem. Phys., 81(6), 2577 (1984).
29. Fraser, G. T., Nelson, D. D. Jr., Charo, A. and Klemperer, W., J. Chem. Phys., 82(6), 2535 (1985).
30. Amos, R. D., Handy, N. C., Knowles, P. J., Rice, J. E. and Stone, A. J., J. Phys. Chem., 89, 2186 (1985).
31. Radom, L., Lathan, W. A., Hehre, W. J. and Pople, J. A., Aust. J. Chem. 25, 1601 (1972).
32. Pople, J. A. and Gordon, M. S., J. Am. Chem. Soc., 89(17), 4253 (1967).
33. Van Alseney, C., Williams, J. O. and Schafer, L., J. Molecular Struct., 76, 179 (1981).
34. Binkley, J. S., Frisch, M. J., DeFrees, D. J., Raghavachari, K., Whiteside, R. A., Schlegel, H. B. and Pople, J. A., Gaussian 82 (Rev. H. 28-Nov. 1983), Carnegie-Mellon University, Pittsburgh, PA 15213.
35. Ditchfield, R., Hehre, W. J. and Pople, J. A., J. Chem. Phys.,

54, 724 (1982).

36. Franci, M. M., Pietro, W. J., Hehre, W. J., Binkley, J. S., Gordon, M. S., DeFrees, J. J. and Pople, J. A., J. Chem. Phys., 77, 3654 (1982).
37. Szabo, A. and Ostlund, N. S., Modern Quantum Chemistry: Introduction to Advanced Electronic Structure Theory, MacMillan Pub. Co., New York, New York 1982, Chapter 3.
38. Moller, C. and Plesset, M. S., Phys. Rev., 46, 628 (1934).
39. Krishnan, R. and Pople, J. A., Int. J. Quantum Chem. Quantum Chem. Symp., 14, 91 (1980).
40. Pople, J. A., Krishnan, R., Schlegel, H. B. and Binkley, J. S., Int. J. Quantum Chem. Quantum Chem. Symp., 13, 225 (1979).
41. Lewis, G. N. and Randall, M., Thermodynamics, revised by Pitzer, K. S. and Brewer, L., McGraw-Hill, New York, New York (1961).
42. Pople, J. A., Schlegel, H. B., Krishnan, R., Defrees, D. J., Binkley, J. S., Frisch, M. J. and Whiteside, R. A., Int. J. Quantum Chem. Quantum Chem. Symp., 15, 269 (1981).
43. Matignon, C. and Frejaques, M., Bull. Soc. Chim., 31, 207 (1922).
44. Wagman, D. D., Evans, W. H., Parker, V. B., Schumm, R. H., Halow, I., Bailey, S. M., Churney, K. L. and Nuttall, R. L., "The NBS Tables of Chemical Thermodynamic Properties: Selected Values for Inorganic and C1 and C2 Organic Substances", J. Chem. Phys. Ref. Data, 11, Suppl. 2 (1982).
45. Sutton, L. E. (Ed.), Tables of Interatomic Distances and Configuration in Molecules and Ions, Chemical Society (London), Burlington House, London (1958).
46. Whiteside, R. A., Frisch, M. J., Binkley, J. S., DeFrees, D. J., Schlegel, H. B., Raghavachari, K. and Pople, J. A., Carnegie-Mellon Quantum Chemistry Archive, 2nd Ed., Department of Chemistry, Carnegie-Mellon University, Pittsburgh PA (1981).
47. Herzberg, G., Molecular Spectra and Molecular Structure I. Spectra of Diatomic Molecules, 2nd Ed., Van Nostrand Reinhold Co., New York, New York (1950).
48. Herzberg, G., Molecular Spectra and Molecular Structure III. Electronic Spectra and Electronic Structure of Polyatomic Molecules, Van Nostrand Reinhold Co., New York, New York (1966).



49. Pople, J. A., Frisch, M. J., Luke, B. T. and Binkley, J. S.,  
Int. J. Quantum Chem. Quantum Chem. Symp., 17, 307 (1983).

VITA

James Ray Diers

Candidate for the Degree of

Master of Science

Thesis: A THEORETICAL STUDY OF CARBAMATE FORMATION

Major Field: Chemistry

Biographical:

Personal Data: Born in Queens, New York, October 28, 1956, the son of Victor and Catherine Diers.

Education: Graduated from Uniondale High School, Uniondale, New York, June, 1974; received Associate of Science degree in Biology from Nassau Community College in May 1976; received Bachelor of Science degree with majors in Biological Sciences and Chemistry from State University of New York at Stony Brook in May 1980; completed requirements for the Master of Science degree at Oklahoma State University in December, 1986.

Professional Experience: Graduate Teaching Assistant, Oklahoma State University, 1980 - 1983; Graduate Research Assistant, Oklahoma State University, 1981, 1983-1986.